

# Differentiating and Integrating ZX Diagrams with Applications to Quantum Machine Learning

Quanlong Wang, Richie Yeung, and Mark Koch

Quantinuum (Cambridge Quantum), UK

ZX-calculus has proved to be a useful tool for quantum technology with a wide range of successful applications. Most of these applications are of an algebraic nature. However, other tasks that involve differentiation and integration remain unreachable with current ZX techniques. Here we elevate ZX to an analytical perspective by realising differentiation and integration entirely within the framework of ZX-calculus. We explicitly illustrate the new analytic framework of ZX-calculus by applying it in context of quantum machine learning for the analysis of barren plateaus.

## 1 Introduction

ZX-calculus is a powerful graphical rewrite system proposed by Coecke and Duncan [10] for linear maps, particularly for quantum circuits. A node with  $n$  edges in a ZX diagram, like in tensor network notation, represent an order  $n$  tensor. Moreover, it is possible to directly evaluate the tensor by performing local rewrites. Using these local rewrites, ZX-calculus has been successfully applied to circuit compilation [4, 5, 17, 38], measurement-based quantum computing [25, 18], fusion-based quantum computing [7], quantum error correction [24, 6], quantum natural language processing [13, 31, 23], and quantum foundations [2, 12, 11, 19]. ZX-calculus can even be used as a concrete realisation of quantum theory [14]. These applications of ZX-calculus are algebraic in nature, and take advantage of *rewriting as a form of computation*: in fact ZX-calculus is a sound, universal [9] and complete [21] proof system that serves as an alternative to traditional linear algebra. However, without the analytical tools of differentiation and integration, ZX-calculus fell short of tackling variational problems such as quantum machine learning or realising a comprehensive version of quantum mechanics including quantum dynamics.

There have been previous attempts at providing for differentiating and integrating ZX diagrams [45, 39, 46]. However, by explicitly using Hilbert space operations, such as addition, these attempts fall outside the realm of vanilla ZX-calculus as there are no techniques on further manipulating sums of diagrams.

In this paper we give for the first time rules for differentiating arbitrary ZX diagrams and integrating a wide class of ZX diagrams (including quantum circuits), thus paving the way for an analytical version of ZX-calculus. We apply these new techniques to develop a framework for a purely ZX-based analysis of the barren plateau phenomenon from quantum machine learning. Furthermore, the results of this paper have been used in [28] to analyse parameter shift rules for gradient computation using ZX.

---

Quanlong Wang: [harny.wang@quantinuum.com](mailto:harny.wang@quantinuum.com)

Richie Yeung: [richie.yeung@quantinuum.com](mailto:richie.yeung@quantinuum.com)

Mark Koch: [mark.koch@quantinuum.com](mailto:mark.koch@quantinuum.com)

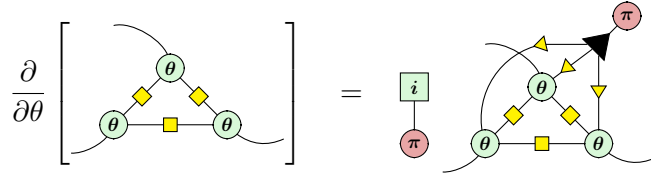


Figure 1: Example of diagrammatic differentiation.

### Summary of results

1. Differentiation of arbitrary (algebraic) ZX diagrams, with a unified diagrammatic chain and product rule. (Theorem 14 and Theorem 16)
2. Definite integration of circuit-like ZX diagrams, with up to 3 occurrences of a parameter. (Proposition 20, Theorem 23, and Theorem 25)
3. Diagrammatic formula for the expectation and variance of a quantum circuit's gradient  $\frac{\partial \langle H \rangle}{\partial \theta_i}$ . (Lemma 29 and Theorem 32)
4. Demonstration of barren plateau analysis for an example ansatz. (Proposition 34)

From a general ZX-calculus perspective, this is the first paper to combine sums of ZX diagrams into a single ZX diagram in a methodical way. In particular, we highlight the importance of the W spider in ZX-calculus, which corresponds to the derivation structure of the product rule. These results required the combined power of the Z, X and W spiders, all of 3 of which can be naturally represented within algebraic ZX-calculus.

**Note:** For presentation purposes, the proofs of some theorems and lemmas are moved to the appendix.

## 2 Algebraic ZX-calculus

The generators of the original ZX-calculus [10] are chosen with the aim to conveniently represent quantum computational models using complementary observables. On the other hand, the ZW-calculus [20] is designed based on the GHZ and W states, two maximally entangled quantum states [15]. It is known that the Z and W spiders from ZW-calculus act as the multiplication and addition monoid respectively, making it possible to perform arithmetic [16, 20].



We will see that the W state is crucial for dealing with sums of diagrams, and it is in fact closely related to the product rule used in differentiation. Conveniently, algebraic ZX-calculus [40] compactly decomposes the W spider and other gadgets such as the logical AND gate [33], into Z spiders, X spiders and triangle gates, thus giving us the benefits of ZX and ZW calculus within a single unified framework.



The yellow triangle of algebraic ZX-calculus is powerful as it sends the computational basis to a non-orthogonal basis, which makes diagrammatic representation and calculation of other logical gates much simpler. Conversely, the representation of the yellow triangle using other graphical calculi is more complicated. Intuitively, this is because the triangle gate is a low-level primitive in comparison to the Z, X, W and H spiders [3]. This algebraic extension of ZX is a universal and complete language for not just complex numbers, but also commutative rings and semirings [42].

In this section, we give an introduction to the algebraic ZX-calculus, including its generators and rewriting rules. In this paper ZX diagrams are either read from left to right or top to bottom.

## 2.1 Generators

The diagrams in algebraic ZX-calculus are defined by freely combining the following generating objects:

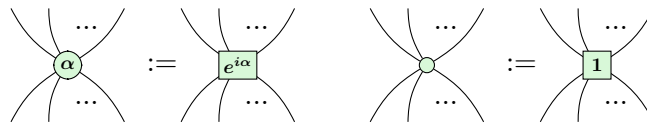
$R_{Z,a}^{(n,m)} : n \rightarrow m$		$\mathbb{I} : 1 \rightarrow 1$	
$H : 1 \rightarrow 1$		$\sigma : 2 \rightarrow 2$	
$C_a : 0 \rightarrow 2$		$C_u : 2 \rightarrow 0$	
$T : 1 \rightarrow 1$		$T^{-1} : 1 \rightarrow 1$	

Table 1: Generators of algebraic ZX-calculus, where  $m, n \in \mathbb{N}$ ,  $a \in \mathbb{C}$ .

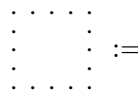
## 2.2 Additional notation

For simplicity, we introduce additional notation based on the given generators:

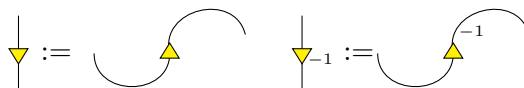
1. The green spider from the original ZX-calculus can be defined using the green box spider in algebraic ZX-calculus.



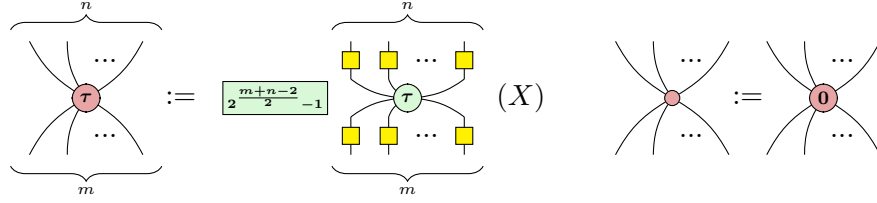
2. The whitespace around a diagram can be interpreted as an explicit horizontal composition with the empty diagram.



3. The transposes of the triangle and the inverse triangle can be drawn as an inverted triangle.

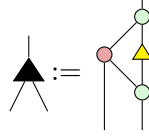


4. The pink spider is the algebraic equivalent of the red spider from the original ZX-calculus. It is only defined for  $\tau \in \{0, \pi\}$ , and is rescaled to have integer components in its matrix representation.



Note that the green box represents the scalar  $\boxed{\frac{m+n-2}{2} \quad -1} = 2^{\frac{m+n-2}{2}}$ .

5. The W spider from ZW-calculus can be expressed as follows.



### 2.3 Interpretation

Although the generators in ZX-calculus are formal mathematical objects in their own right, in the context of this paper we interpret the generators as linear maps, so each ZX diagram is equivalent to a vector or matrix. For  $a \in \mathbb{C}$  and  $\alpha \in \mathbb{R}$ , we have

$$\begin{array}{c} \overbrace{\quad \quad \quad}^n \\ \diagdown \quad \diagup \\ \quad \quad \quad \\ \diagup \quad \diagdown \\ \underbrace{\quad \quad \quad}_m \end{array} \begin{array}{c} \boxed{a} \\ \quad \quad \quad \end{array} = |0\rangle^{\otimes m} \langle 0|^{\otimes n} + a |1\rangle^{\otimes m} \langle 1|^{\otimes n}, \quad (Z)$$

$$\begin{array}{c} \overbrace{\quad \quad \quad}^n \\ \diagdown \quad \diagup \\ \quad \quad \quad \\ \diagup \quad \diagdown \\ \underbrace{\quad \quad \quad}_m \end{array} \begin{array}{c} \boxed{k\pi} \\ \quad \quad \quad \end{array} = \sum_{\substack{0 \leq i_1, \dots, i_m, j_1, \dots, j_n \leq 1 \\ i_1 + \dots + i_m + k \equiv j_1 + \dots + j_n \pmod{2}}} |i_1, \dots, i_m\rangle \langle j_1, \dots, j_n|, \quad k \in \{0, 1\},$$

$$\begin{array}{c} \boxed{\quad} \\ | \\ \quad \quad \quad \end{array} = \frac{1}{\sqrt{2}} \begin{pmatrix} 1 & 1 \\ 1 & -1 \end{pmatrix}, \quad \begin{array}{c} \triangle \\ | \\ \quad \quad \quad \end{array} = \begin{pmatrix} 1 & 1 \\ 0 & 1 \end{pmatrix}, \quad \begin{array}{c} \triangle^{-1} \\ | \\ \quad \quad \quad \end{array} = \begin{pmatrix} 1 & -1 \\ 0 & 1 \end{pmatrix}$$

$$\begin{array}{c} \boxed{\alpha} \\ \triangle \\ \boxed{\quad} \\ | \\ \quad \quad \quad \end{array} = e^{i\frac{\alpha}{2}} \begin{pmatrix} \cos \frac{\alpha}{2} & -i \sin \frac{\alpha}{2} \\ -i \sin \frac{\alpha}{2} & \cos \frac{\alpha}{2} \end{pmatrix},$$

$$\begin{array}{c} \circ \\ | \\ \quad \quad \quad \end{array} = \begin{pmatrix} 0 & 1 \\ 1 & 0 \end{pmatrix}, \quad \begin{array}{c} \circ \\ \boxed{a} \\ | \\ \quad \quad \quad \end{array} = \boxed{a-1} = a, \quad \begin{array}{c} \circ \\ | \\ \quad \quad \quad \end{array} = 0, \quad \begin{array}{c} | \\ \quad \quad \quad \end{array} = \begin{pmatrix} 1 & 0 \\ 0 & 1 \end{pmatrix},$$

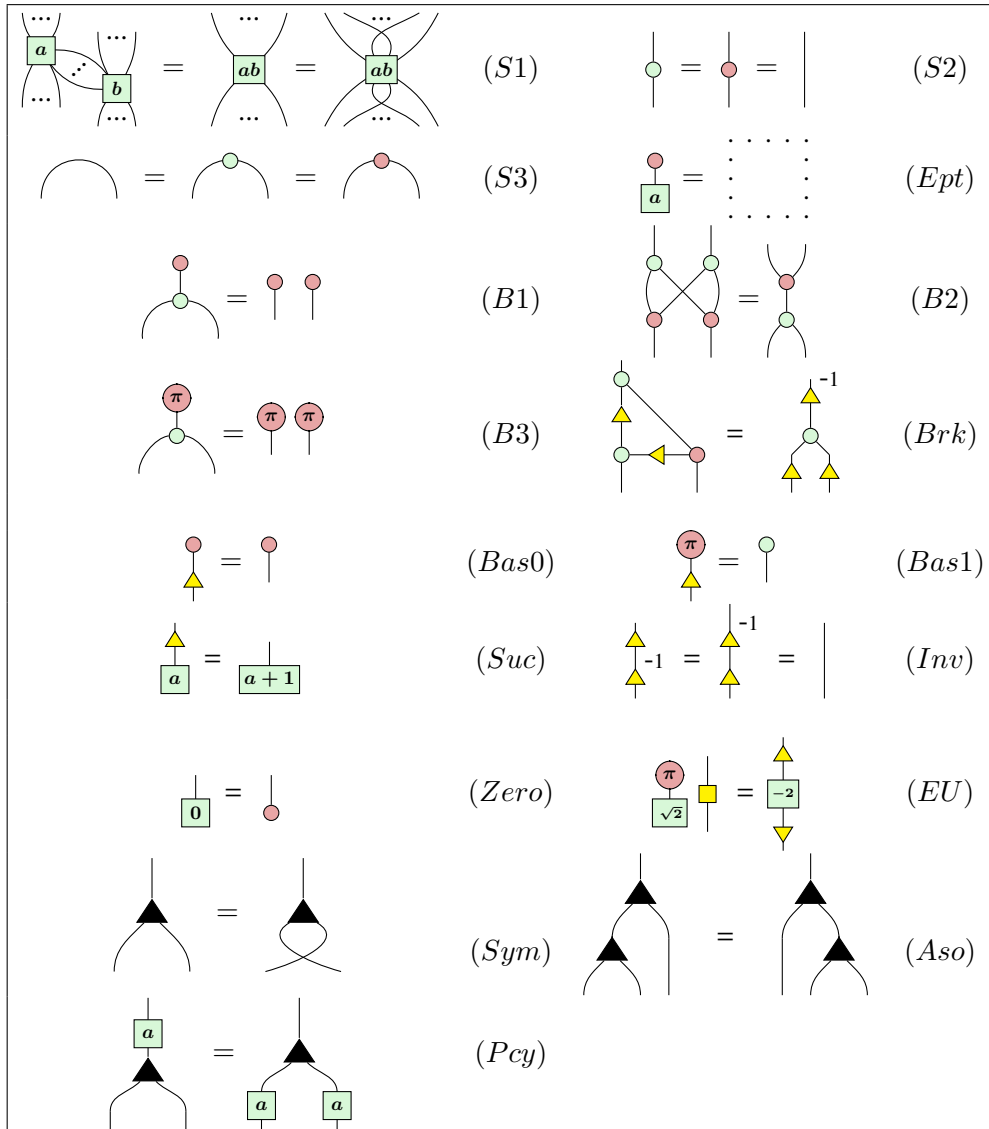
$$\begin{matrix} \diagup \diagdown \\ \diagdown \diagup \end{matrix} = \begin{pmatrix} 1 & 0 & 0 & 0 \\ 0 & 0 & 1 & 0 \\ 0 & 1 & 0 & 0 \\ 0 & 0 & 0 & 1 \end{pmatrix}, \quad \frown = \begin{pmatrix} 1 \\ 0 \\ 0 \\ 1 \end{pmatrix}, \quad \smile = \begin{pmatrix} 1 & 0 & 0 & 1 \end{pmatrix}, \quad \begin{matrix} \cdots \\ \cdots \\ \cdots \\ \cdots \end{matrix} = 1,$$

where

$$|0\rangle = \begin{pmatrix} 1 \\ 0 \end{pmatrix} = \begin{matrix} \bullet \\ | \end{matrix}, \quad \langle 0| = \begin{pmatrix} 1 & 0 \end{pmatrix} = \begin{matrix} | \\ \bullet \end{matrix}, \quad |1\rangle = \begin{pmatrix} 0 \\ 1 \end{pmatrix} = \begin{matrix} \pi \\ | \end{matrix}, \quad \langle 1| = \begin{pmatrix} 0 & 1 \end{pmatrix} = \begin{matrix} | \\ \pi \end{matrix}.$$

## 2.4 Rules

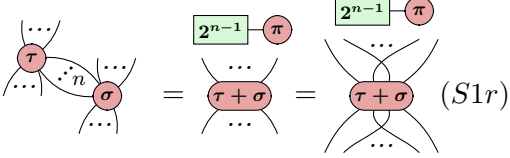
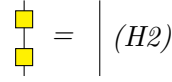
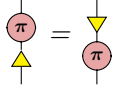
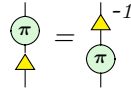
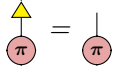
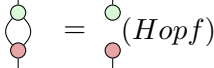
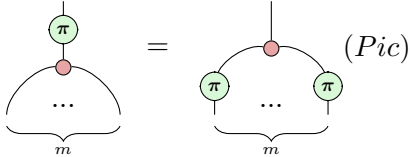
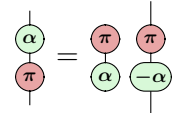
Now we give the rewriting rules of algebraic ZX-calculus.



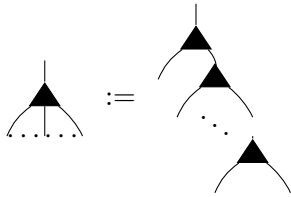
Where  $a, b \in \mathbb{C}$ . The vertically flipped versions of the rules are assumed to hold as well.

## 2.5 Useful lemmas

The following lemmas which will be used in the sequel can be derived from the rules.

<p><b>Lemma 1.</b> [41] For <math>\tau, \sigma \in \{0, \pi\}</math>, pink spiders fuse.</p> 	<p><b>Lemma 2.</b> [41] Hadamard is involutive.</p> 
<p><b>Lemma 3.</b> [41] Pink <math>\pi</math> transposes the triangle.</p> 	<p><b>Lemma 4.</b> [41] Green <math>\pi</math> inverts the triangle.</p> 
<p><b>Lemma 5.</b> [41] triangle stabilises <math>\langle 1 </math>.</p> 	<p><b>Lemma 6.</b> [41] Hopf rule.</p> 
<p><b>Lemma 7.</b> [41] <math>\pi</math> copy rule. For <math>m \geq 0</math>:</p> 	<p><b>Lemma 8.</b> [41] <math>\pi</math> commutation rule.</p> 

**Remark 9.** Due to the associative rule (Aso), we can define the  $W$  spider



and give its interpretation as follows [43]:

$$\underbrace{\text{W spider}}_m = \underbrace{|0 \cdots 0\rangle}_m \langle 0| + \sum_{k=1}^m \underbrace{|0 \cdots 0 1 0 \cdots 0\rangle}_{k-1} \langle 1|.$$

As a consequence, we have

$$\begin{aligned}
 \text{Spider with } \pi \text{ on top} &= \text{Vertical line with } \pi \text{ on top} \\
 \text{Spider with } \pi \text{ on top} &= \text{Sum of diagrams with } \pi \text{ on top and bottom legs}
 \end{aligned}
 \tag{1}$$

For  $n = 2$ , the state  $|01\rangle + |10\rangle$  can be represented as the quantum state corresponding to the Pauli X gate according to the map-state duality:

**Lemma 10.**

$$\text{Spider with } \pi \text{ on top} = \text{Spider with } \pi \text{ on bottom}$$

### 3 Differentiating ZX diagrams

In this section, we show how to differentiate any algebraic ZX diagram within algebraic ZX-calculus, and how to represent the derivative of original ZX diagrams [10] and quantum circuits in algebraic ZX as a special case. We refer to [39] for a formal definition of the categorical semantics of diagrammatic differentiation. We start by differentiating the simplest parameterised generator in original ZX-calculus: the one-legged green spider.

**Lemma 11.** *Suppose  $f(\theta)$  is a differentiable real function of  $\theta$ . Then*

$$\frac{\partial}{\partial \theta} \left[ \text{Spider with } f(\theta) \text{ on top} \right] = \text{Spider with } if'(\theta) \text{ on top and } \pi \text{ on bottom}$$

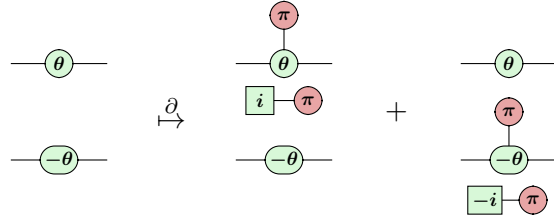
**Note:** For presentation purposes, the proofs of some theorems and lemmas are moved to the appendix.

Using the derivative of the one-legged spider, we can differentiate any ZX diagram with only one occurrence of the parameter being differentiated against. Here is an example.

$$\text{Diagram with } 2\theta \text{ on top} = \text{Diagram with } 2\theta \text{ on top} \xrightarrow{\partial} \text{Diagram with } \pi \text{ on top and } 2i \text{ on bottom} \stackrel{B3}{=} \text{Diagram with } \pi \text{ on top and } 2i \text{ on bottom}$$

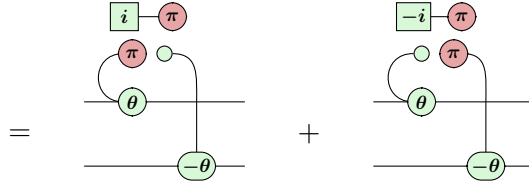
$$|00\rangle \langle 0| + e^{i2\theta} |11\rangle \langle 1| \xrightarrow{\partial} 2i * e^{i2\theta} |11\rangle \langle 1|$$

When there are multiple occurrences of the same parameter, the derivative can be expressed as a sum of ZX diagrams using the product rule. For example, the density matrix of  $R_z(\theta)$  can be differentiated as follows.

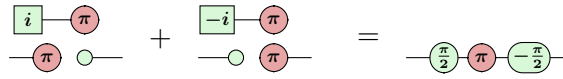


Since there are no rules on how to further manipulate sums of ZX diagrams, we cannot do much with derivatives in this form. Moreover, the addition operation is discouraged in ZX-calculus as it does not have a meaningful temporal interpretation, whilst the composition of two diagrams  $f \circ g$  can be interpreted as two processes happening one after the other, and the tensor of two diagram  $f \otimes g$  can be interpreted as two processes happening concurrently.

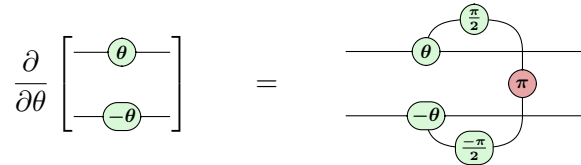
For these reasons, we should try to express the derivative as a single diagram. By observing that the product rule leaves the unparameterised parts of the diagram untouched and can be “factored out”, we only need to resynthesise the derivative of the parameterised part.



After this factorisation, the diagrammatic terms in the sum (top of the diagram) can be further manipulated until we can eliminate the sum using a simple rule such as  $|0\rangle + |1\rangle = \sqrt{2}|+\rangle$ . (See appendix for a demonstration of this technique)



Therefore



This equation, first derived by Zhao et al. [46], is essentially the parameter shift rule by Schuld et al. [35] expressed as a single ZX diagram (also see Corollary 18).

The key result of the paper allows us to express the derivative of an arbitrary ZX diagram in terms of a single diagram. It is based on the observation that the product rule and the unnormalised  $|W_n\rangle$  state resemble each other: in the product rule, each term has one differentiated function, and in the W state each term has one bit set to 1 in the basis state.

$$\partial(fgh) = (\partial f)gh + f(\partial g)h + fg(\partial h)$$

$$|W_3\rangle = |100\rangle + |010\rangle + |001\rangle$$

We will show in Theorem 16 that the product rule can indeed be represented using a W state supplemented with some local change of bases. The following lemma demonstrates that the difference between  $f$  and  $\partial f$  can be expressed as a change of basis from the computational basis  $|0\rangle, |1\rangle$ .

**Lemma 12.** For any complex number  $a$ , we have



To differentiate algebraic ZX diagrams, we first differentiate its parameterised generator, the one-legged green box:

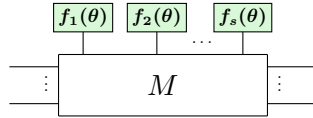
**Lemma 13.** *Suppose  $f : \mathbb{R} \rightarrow \mathbb{C}$  is a differentiable function. If  $f(\theta) \neq 0$  for all  $\theta \in \mathbb{R}$ , then*

$$\frac{\partial}{\partial \theta} \left[ \begin{array}{c} \boxed{f(\theta)} \\ | \\ \text{---} \end{array} \right] = \begin{array}{c} \boxed{\frac{f'(\theta)}{f(\theta)}} \\ | \\ \text{---} \end{array} \begin{array}{c} \pi \\ | \\ \text{---} \end{array} \begin{array}{c} \boxed{f(\theta)} \\ | \\ \text{---} \end{array}$$

If  $f(\theta_0) = 0$  for some  $\theta_0 \in \mathbb{R}$ , then

$$\frac{\partial}{\partial \theta} \left[ \begin{array}{c} \boxed{f(\theta)} \\ | \\ \text{---} \end{array} \right]_{\theta_0} = \begin{array}{c} \pi \\ | \\ \boxed{f'(\theta_0)} \\ | \\ \text{---} \end{array}$$

All parameterised differentiable algebraic ZX diagrams can be rewritten into the following form, where  $M$  is an unparameterised ZX diagram with respect to  $\theta$ , and  $\{f_i(\theta)\}_i$  are differentiable real functions of  $\theta$ . Parameterised green spiders can be written as a green box with an exponentiated phase, and parameterised red spiders can be converted to parameterised green spiders via Hadamard conjugation. We emphasise that  $M$  can contain other parameterised spiders, just not with respect to  $\theta$ .



**Theorem 14.** *Assume  $f_j : \mathbb{R} \rightarrow \mathbb{C}$  are differentiable functions. If  $f_j(\theta) \neq 0$  for all  $\theta \in \mathbb{R}$  and  $j \in \{1, \dots, s\}$  then*

$$\frac{\partial}{\partial \theta} \left[ \begin{array}{c} \boxed{f_1(\theta)} \quad \boxed{f_2(\theta)} \quad \dots \quad \boxed{f_s(\theta)} \\ | \quad | \quad \dots \quad | \\ \text{---} \\ \boxed{M} \\ \text{---} \\ | \quad | \quad \dots \quad | \end{array} \right] = \begin{array}{c} \pi \\ \blacktriangle \\ \begin{array}{c} \boxed{\frac{f'_1(\theta)}{f_1(\theta)}} \quad \boxed{\frac{f'_2(\theta)}{f_2(\theta)}} \quad \dots \quad \boxed{\frac{f'_s(\theta)}{f_s(\theta)}} \\ | \quad | \quad \dots \quad | \\ \text{---} \\ \boxed{f_1(\theta)} \quad \boxed{f_2(\theta)} \quad \dots \quad \boxed{f_s(\theta)} \\ | \quad | \quad \dots \quad | \\ \text{---} \\ \boxed{M} \\ \text{---} \\ | \quad | \quad \dots \quad | \end{array} \end{array}$$

If for some  $\theta_0$ , we have  $f_j(\theta_0) \neq 0$  for  $1 \leq j \leq k$  and  $f_j(\theta_0) = 0$  for  $k+1 \leq j \leq s$  (the order of the functions can be changed without loss of generality), then

$$\frac{\partial}{\partial \theta} \left[ \begin{array}{c} \boxed{f_1(\theta)} \quad \boxed{f_2(\theta)} \quad \dots \quad \boxed{f_s(\theta)} \\ | \quad | \quad \dots \quad | \\ \text{---} \\ \boxed{M} \\ \text{---} \\ | \quad | \quad \dots \quad | \end{array} \right]_{\theta_0} = \begin{array}{c} \pi \\ \blacktriangle \\ \begin{array}{c} \boxed{\frac{f'_1(\theta_0)}{f_1(\theta_0)}} \quad \boxed{\frac{f'_k(\theta_0)}{f_k(\theta_0)}} \quad \boxed{f'_{k+1}(\theta_0)} \quad \boxed{f'_s(\theta_0)} \\ | \quad | \quad \dots \quad | \\ \text{---} \\ \boxed{f_1(\theta_0)} \quad \boxed{f_k(\theta_0)} \quad \dots \quad \text{---} \\ | \quad | \quad \dots \quad | \\ \text{---} \\ \boxed{M} \\ \text{---} \\ | \quad | \quad \dots \quad | \end{array} \end{array}$$

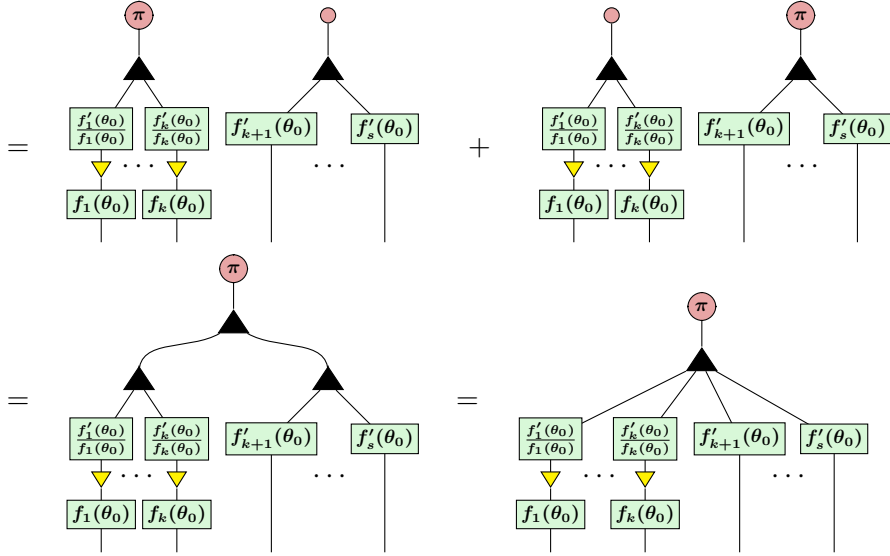
*Proof.* By linearity, differentiating the overall diagram amounts to differentiating the parameterised part of the diagram:

$$\begin{aligned}
& \frac{\partial}{\partial \theta} \left[ \begin{array}{c} \boxed{f_1(\theta)} \quad \boxed{f_2(\theta)} \quad \boxed{f_s(\theta)} \\ | \quad | \quad \dots \quad | \end{array} \right] \\
&= \begin{array}{c} \boxed{\frac{f'_1(\theta)}{f_1(\theta)}} \quad \pi \\ | \quad | \\ \pi \quad \boxed{f_1(\theta)} \quad \boxed{f_2(\theta)} \quad \boxed{f_s(\theta)} \\ | \quad | \quad \dots \quad | \end{array} + \begin{array}{c} \boxed{\frac{f'_2(\theta)}{f_2(\theta)}} \quad \pi \\ | \quad | \\ \pi \quad \boxed{f_1(\theta)} \quad \boxed{f_2(\theta)} \quad \boxed{f_s(\theta)} \\ | \quad | \quad \dots \quad | \end{array} + \dots + \begin{array}{c} \boxed{\frac{f'_s(\theta)}{f_s(\theta)}} \quad \pi \\ | \quad | \\ \pi \quad \boxed{f_1(\theta)} \quad \boxed{f_2(\theta)} \quad \boxed{f_s(\theta)} \\ | \quad | \quad \dots \quad | \end{array} \\
&= \begin{array}{c} \boxed{\frac{f'_1(t)}{f_1(t)}} \quad \pi \\ | \quad | \\ \pi \quad \boxed{f_1(t)} \quad \boxed{f_2(t)} \quad \boxed{f_s(t)} \\ | \quad | \quad \dots \quad | \end{array} + \begin{array}{c} \boxed{\frac{f'_2(t)}{f_2(t)}} \quad \pi \\ | \quad | \\ \pi \quad \boxed{f_1(t)} \quad \boxed{f_2(t)} \quad \boxed{f_s(t)} \\ | \quad | \quad \dots \quad | \end{array} + \dots + \begin{array}{c} \boxed{\frac{f'_s(t)}{f_s(t)}} \quad \pi \\ | \quad | \\ \pi \quad \boxed{f_1(t)} \quad \boxed{f_2(t)} \quad \boxed{f_s(t)} \\ | \quad | \quad \dots \quad | \end{array} \\
&= \begin{array}{c} \pi \\ | \quad | \quad | \\ \boxed{\frac{f'_1(\theta)}{f_1(\theta)}} \quad \boxed{\frac{f'_2(\theta)}{f_2(\theta)}} \quad \boxed{\frac{f'_s(\theta)}{f_s(\theta)}} \\ | \quad | \quad \dots \quad | \\ \boxed{f_1(\theta)} \quad \boxed{f_2(\theta)} \quad \boxed{f_s(\theta)} \end{array} + \begin{array}{c} \pi \\ | \quad | \quad | \\ \boxed{\frac{f'_1(\theta)}{f_1(\theta)}} \quad \boxed{\frac{f'_2(\theta)}{f_2(\theta)}} \quad \boxed{\frac{f'_s(\theta)}{f_s(\theta)}} \\ | \quad | \quad \dots \quad | \\ \boxed{f_1(\theta)} \quad \boxed{f_2(\theta)} \quad \boxed{f_s(\theta)} \end{array} + \dots + \begin{array}{c} \pi \\ | \quad | \quad | \\ \boxed{\frac{f'_1(\theta)}{f_1(\theta)}} \quad \boxed{\frac{f'_2(\theta)}{f_2(\theta)}} \quad \boxed{\frac{f'_s(\theta)}{f_s(\theta)}} \\ | \quad | \quad \dots \quad | \\ \boxed{f_1(\theta)} \quad \boxed{f_2(\theta)} \quad \boxed{f_s(\theta)} \end{array} \\
&= \begin{array}{c} \pi \\ | \quad | \quad | \\ \boxed{\frac{f'_1(\theta)}{f_1(\theta)}} \quad \boxed{\frac{f'_2(\theta)}{f_2(\theta)}} \quad \boxed{\frac{f'_s(\theta)}{f_s(\theta)}} \\ | \quad | \quad \dots \quad | \\ \boxed{f_1(\theta)} \quad \boxed{f_2(\theta)} \quad \boxed{f_s(\theta)} \end{array}
\end{aligned}$$

The first step follows from Lemma 13 and the product rule, and the second step performs further factorisation of the diagram. The third step follows from Lemma 12. The final step uses the property of W spider as given in (1).

If  $f_j(\theta_0) \neq 0$  for  $1 \leq j \leq k$  and  $f_j(\theta_0) = 0$  for  $k+1 \leq j \leq s$  (the order of the functions can be changed without loss of generality), then the diagram can be differentiated in two parts using the product rule:

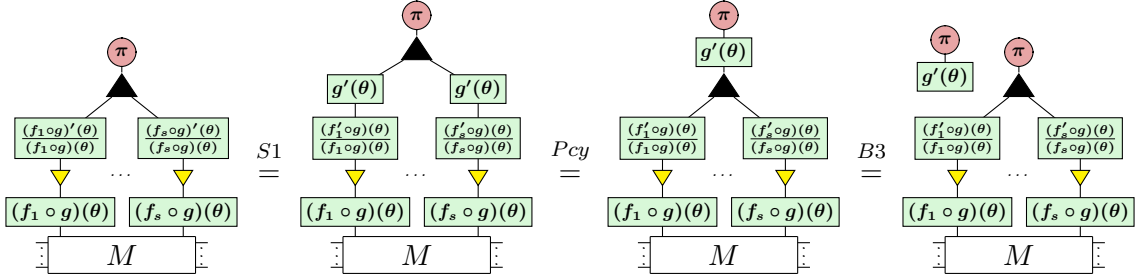
$$\begin{aligned}
& \frac{\partial}{\partial \theta} \left[ \begin{array}{c} \boxed{f_1(\theta)} \quad \boxed{f_2(\theta)} \quad \boxed{f_s(\theta)} \\ | \quad | \quad \dots \quad | \end{array} \right]_{\theta_0} \\
&= \frac{\partial}{\partial \theta} \left[ \begin{array}{c} \boxed{f_1(\theta)} \quad \boxed{f_k(\theta)} \\ | \quad \dots \quad | \end{array} \right]_{\theta_0} \left[ \begin{array}{c} \boxed{f_{k+1}(\theta)} \quad \boxed{f_s(\theta)} \\ | \quad \dots \quad | \end{array} \right]_{\theta_0} + \left[ \begin{array}{c} \boxed{f_1(\theta)} \quad \boxed{f_k(\theta)} \\ | \quad \dots \quad | \end{array} \right]_{\theta_0} \frac{\partial}{\partial \theta} \left[ \begin{array}{c} \boxed{f_{k+1}(\theta)} \quad \boxed{f_s(\theta)} \\ | \quad \dots \quad | \end{array} \right]_{\theta_0} \\
&= \frac{\partial}{\partial \theta} \left[ \begin{array}{c} \boxed{f_1(\theta)} \quad \boxed{f_k(\theta)} \\ | \quad \dots \quad | \end{array} \right]_{\theta_0} \begin{array}{c} \bullet \quad \bullet \\ | \quad | \end{array} \\
&+ \left[ \begin{array}{c} \boxed{f_1(\theta_0)} \quad \boxed{f_k(\theta_0)} \\ | \quad \dots \quad | \end{array} \right] \left[ \begin{array}{c} \pi \\ | \quad | \quad | \\ \boxed{f'_{k+1}(\theta_0)} \quad \boxed{f'_{k+2}(\theta_0)} \quad \boxed{f'_s(\theta_0)} \\ | \quad \dots \quad | \end{array} + \dots + \begin{array}{c} \bullet \quad \bullet \quad \pi \\ | \quad | \quad | \\ \boxed{f'_{k+1}(\theta_0)} \quad \boxed{f'_{k+2}(\theta_0)} \quad \boxed{f'_s(\theta_0)} \\ | \quad \dots \quad | \end{array} \right]
\end{aligned}$$



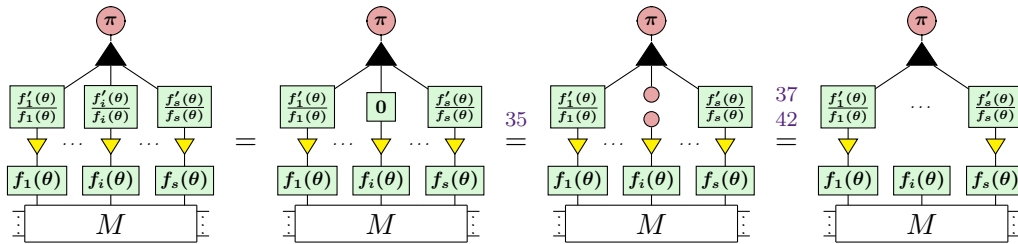
□

This theorem unifies the linearity and product rules of differential calculus into a single diagram, without a blowup in diagram size: the number of nodes added to the diagram after differentiation is linearly proportional to the number of parameter occurrences. This makes the result practically useful for both calculations by hand and computer simulation.

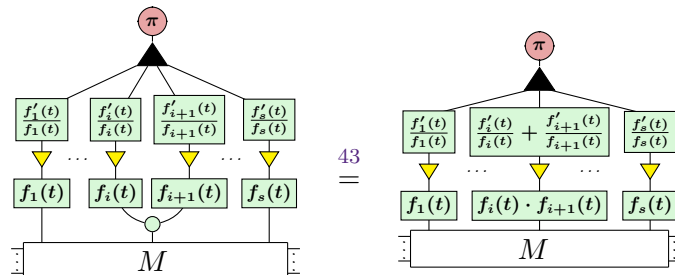
**Remark 15.** We can use this representation of derivatives to graphically prove properties of differential calculus. For example, we get a diagrammatic version of the chain rule:



If  $f_i$  is a constant function, the corresponding spider does not contribute to the derivative:

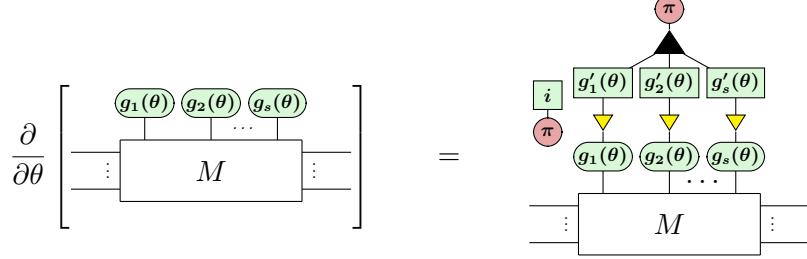


Finally, the differentiation gadget nicely interacts with spider fusion:



Diagrammatic differentiation for regular ZX diagrams corresponds to the special case where all  $f_j$  are phase functions:

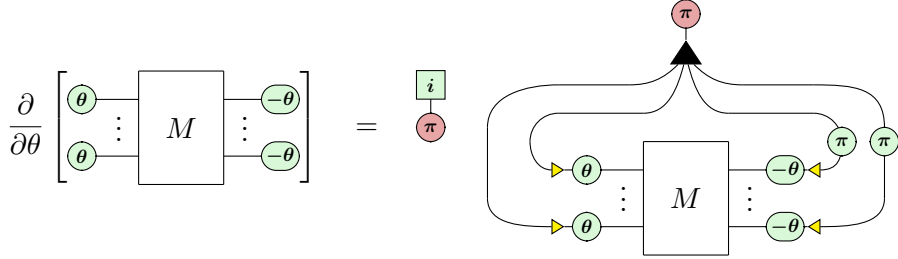
**Theorem 16.** *The derivative of a differentiable ZX diagram can be expressed as a single ZX diagram:*



*Proof.* This is a special case of Theorem 14, where  $f_j(\theta) = e^{ig_j(\theta)}$  and  $\frac{f'_j(\theta)}{f_j(\theta)} = ig'_j(\theta)$ . The “ $i$ ” is common across all functions and can be factored out through the W spider using the diagrammatic chain rule from Remark 15.  $\square$

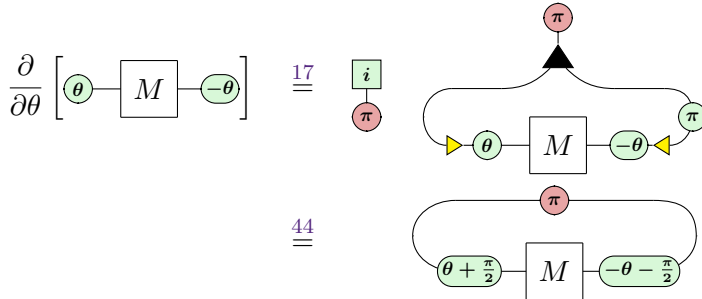
Since we can now differentiate arbitrary ZX diagrams, we can consider differentiating quantum circuits as a special case of Theorem 16. Executing a circuit on a quantum computer estimates the expectation value  $\langle H \rangle = \langle 0 | U^\dagger(\theta) H U(\theta) | 0 \rangle$ . Thus, the ZX diagram representing  $\langle H \rangle$  has an equal number of occurrences of  $\theta$  and  $-\theta$ .

**Corollary 17.** *The derivative of a parameterised quantum circuit can be expressed as a single ZX diagram:*



*Proof.* Noting that  $\frac{\partial}{\partial \theta} -\theta = -1$  and  $\boxed{-1} = \pi$ , this follows directly from Theorem 16.  $\square$

**Corollary 18.** *As a special case of Corollary 17, we obtain the parameter-shift rule from [35].*



**Remark 19.** *This result has been given as a theorem in [46], here we directly get it as a consequence of Corollary 17 which follows from Theorem 16.*

From Corollary 17, we thus have a simple diagrammatic expression for the derivative of any parameterised quantum circuit. In general, it is not easy to obtain the derivative of a parametrised matrix in a single term bra-ket expression (with no sums, e.g.  $\langle \phi | ABC | \psi \rangle$ ), thus showing the power of ZX-calculus and 2-dimensional diagrammatic reasoning.

Similar to how the decomposition of the Pauli X gate in Corollary 18 gives us a 2-term parameter shift rule, decompositions of the  $W$  state in Corollary 17 are used in [28] to obtain shift rules for gates with an arbitrary number of  $\theta$ -occurrences in particular generalising the existing shift rules from [35] and [1]. Furthermore, they use the analytical ZX technology developed here to prove the optimality of the shift rule given in [1].

## 4 Integrating ZX diagrams

In this section we show how to integrate a wide class of ZX diagrams using algebraic ZX-calculus. This allows us to evaluate the expectation and variance of a quantum circuit's derivative over the uniform distribution, as demonstrated in section 5.

**Proposition 20.** *Let  $k$  be an arbitrary non-zero integer,  ${}^{m+1}\left\{ \begin{array}{c} \vdots \\ K \\ \vdots \end{array} \right\}^{n+1}$  be any ZX diagram with  $m, n \geq 0$  which has no occurrence of  $\alpha$ . Then*

$$\frac{1}{2\pi} \int_{-\pi}^{\pi} {}^m \left\{ \begin{array}{c} \overset{k\alpha}{\vdots} \\ K \\ \underset{-k\alpha}{\vdots} \end{array} \right\}^n d\alpha = {}^m \left\{ \begin{array}{c} \vdots \\ K \\ \vdots \end{array} \right\}^n$$

**Remark 21.** *This proposition has been proved in [46] for  $k = 1$ , here we give a new proof with our sum techniques.*

**Remark 22.** *Note that the results in this section are also applicable in cases where the number of positive and negative occurrences of  $k\alpha$  are different. We achieve this by adding a pink dummy spider:*

$$\frac{1}{2\pi} \int_{-\pi}^{\pi} {}^m \left\{ \begin{array}{c} \overset{k\alpha}{\vdots} \\ K \\ \underset{-k\alpha}{\vdots} \end{array} \right\}^n d\alpha = \frac{1}{2\pi} \int_{-\pi}^{\pi} {}^m \left\{ \begin{array}{c} \overset{k\alpha}{\vdots} \\ K \\ \underset{-k\alpha}{\vdots} \end{array} \right\}^n d\alpha \stackrel{20}{=} {}^m \left\{ \begin{array}{c} \vdots \\ K \\ \vdots \end{array} \right\}^n$$

**Theorem 23.** *Let  $k$  be an arbitrary non-zero integer,  ${}^{m+2}\left\{ \begin{array}{c} \vdots \\ A \\ \vdots \end{array} \right\}^{n+2}$  be any ZX diagram with  $m, n \geq 0$  which has no occurrence of  $\alpha$ . Then*

$$\frac{1}{2\pi} \int_{-\pi}^{\pi} {}^m \left\{ \begin{array}{c} \overset{k\alpha}{\vdots} \\ A \\ \underset{-k\alpha}{\vdots} \end{array} \right\}^n d\alpha =$$

**Remark 24.** The corresponding result of this theorem is shown as Lemma 2 in [46] where there are three diagrammatic sum terms after integration, which results in their computation of variance of gradients becoming very complicated. Here we only obtain a single diagram after integration.

**Theorem 25.** Let  $k$  be an arbitrary non-zero integer,  ${}_{m+3} \left\{ \begin{array}{c} \vdots \\ A \\ \vdots \end{array} \right\}_{n+3}$  be any ZX diagram with  $m, n \geq 0$  which has no occurrence of  $\alpha$ . Then

$$\frac{1}{2\pi} \int_{-\pi}^{\pi} \left( \begin{array}{c} (k\alpha) \\ (k\alpha) \\ (k\alpha) \\ \vdots \\ A \\ \vdots \\ (-k\alpha) \\ (-k\alpha) \\ (-k\alpha) \end{array} \right)_n d\alpha = \left( \begin{array}{c} \text{Diagram with } m \text{ inputs and } n \text{ outputs, } A \text{ box, and } \alpha \text{ nodes} \end{array} \right)_n$$

**Remark 26.** Note that the constructions described here do not immediately generalise to diagrams with more than three positive and negative parameter occurrences.

The proofs for Theorem 23 and Theorem 25 are similar to Theorem 20, and are given in the appendix.

## 5 Example Application: Quantum Machine Learning

In the NISQ era of quantum computing [34], many applications require the optimisation of parameterised quantum circuits: in quantum chemistry, variational quantum eigensolvers [30] are optimised to find the ground state of a Hamiltonian; in quantum machine learning, a circuit ansatz is optimised against a cost function [29], much alike how neural networks are optimised in classical machine learning.

However, while the approach of using gradient-based methods to optimise deep neural networks has been consistently effective [8], gradient-based optimisation of parameterised quantum circuits often suffer from barren plateaus: the training landscape of many circuit ansätze have been shown to be exponentially flat with respect to circuit size, making gradient descent impossible [32]. Therefore, it is crucial to develop techniques to detect and avoid barren plateaus.

So far, there has not been a fully diagrammatic analysis of barren plateaus using ZX-calculus. We believe the main obstacle to the analysis is the lack of techniques for manipulating sums of diagrams: an expectation of a Hamiltonian contains at least two occurrences of each circuit parameter, so the derivative of the expectation with respect to that parameter requires the product rule. Similarly, the rule for integrating diagrams in [46] introduces three terms, after  $n$  integrals there would be  $3^n$  terms. Using these rules, the analysis of barren plateaus become exponentially costly, as the number of diagrams to be evaluated is exponential to the number of parameters in the circuit.

In this section, as a demonstration of the new differentiation and integration techniques of this paper, we show that the analysis of barren plateaus by Zhao et al. [46] can be done entirely within the framework of ZX without introducing sums of diagrams. Using the same setup, we consider an  $n$ -qubit parameterised quantum circuit  $U(\theta)$  and a Hamiltonian  $H$ , then the expectation of  $H$

can be written as  $\langle H \rangle = \langle 0 | U^\dagger(\boldsymbol{\theta}) H U(\boldsymbol{\theta}) | 0 \rangle$ , where the variables of the parameterised quantum circuit appear exactly once in  $U(\boldsymbol{\theta})$ . The parameters of the quantum circuit are assumed to be independently and uniformly distributed on the interval  $[\pi, -\pi]$ , as this is a common way to initialise parameters. If  $\mathbf{Var} \left( \frac{\partial \langle H \rangle}{\partial \theta_j} \right) \approx 0$ , then the quantum circuit is likely to start in a barren plateau where the circuit gradient  $\frac{\partial \langle H \rangle}{\partial \theta_j}$  is close to 0.

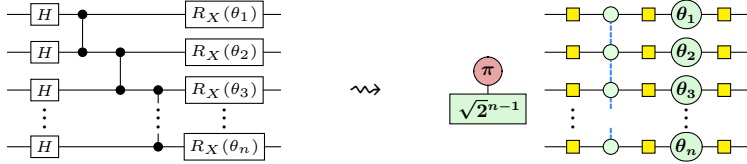
We can represent the gate set as follows:

$$R_Z(\theta) = \text{---} \textcircled{\theta} \text{---}, \quad R_X(\theta) = \text{---} \textcircled{\theta} \text{---}, \quad CNOT = \begin{array}{c} \text{---} \textcircled{\phantom{\theta}} \text{---} \\ | \\ \text{---} \textcircled{\phantom{\theta}} \text{---} \end{array}, \quad CZ = \begin{array}{c} \text{---} \textcircled{\pi} \text{---} \\ | \\ \text{---} \textcircled{\sqrt{2}} \text{---} \end{array},$$

$$H = \frac{1}{\sqrt{2}} \begin{pmatrix} 1 & 1 \\ 1 & -1 \end{pmatrix} = \text{---} \textcircled{\phantom{\theta}} \text{---}$$

We use blue dashed lines  $\text{---} \text{---} \text{---}$  to denote wires  $\text{---} \textcircled{\phantom{\theta}} \text{---}$  with a Hadamard gate on them.

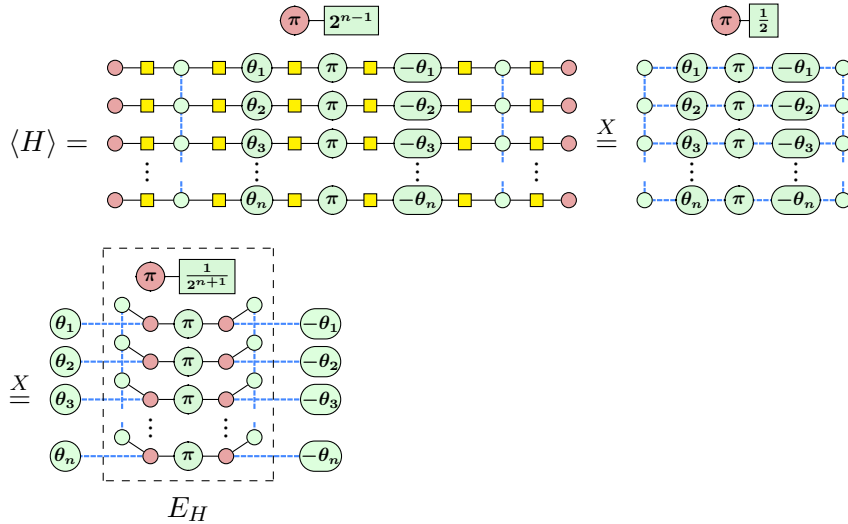
**Example 27.** The ZX representation of the following ansatz from [37] is given below.



Given an ansatz  $U(\boldsymbol{\theta})$  and a Hamiltonian  $H$ , we use the following notation to denote diagrams for the expectation value  $\langle H \rangle = \langle 0 | U^\dagger(\boldsymbol{\theta}) H U(\boldsymbol{\theta}) | 0 \rangle$  where the parametrised spiders are fused out:

$$\langle H \rangle = \begin{array}{c} \textcircled{\theta_1} \\ \vdots \\ \textcircled{\theta_m} \end{array} \text{---} E_H \text{---} \begin{array}{c} \textcircled{-\theta_1} \\ \vdots \\ \textcircled{-\theta_m} \end{array} \quad (2)$$

**Example 28.** For the ansatz from Example 27 and the Hamiltonian  $H = Z^{\otimes n}$  we have

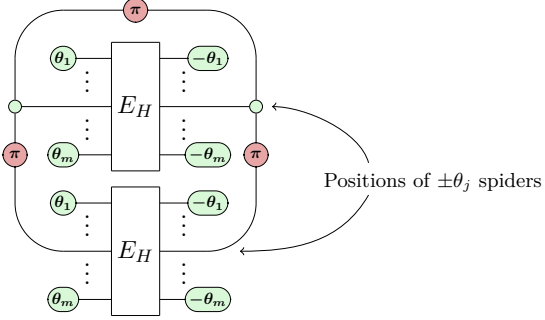


**Lemma 29.** Given  $\langle H \rangle$  in the form of (2), we have  $\mathbf{E} \left( \frac{\partial \langle H \rangle}{\partial \theta_j} \right) = 0$ , for  $j = 1, \dots, m$ .

As a consequence, we have

$$\begin{aligned} \text{Var} \left( \frac{\partial \langle H \rangle}{\partial \theta_j} \right) &= \mathbf{E} \left( \left( \frac{\partial \langle H \rangle}{\partial \theta_j} \right)^2 \right) \\ &= \frac{1}{(2\pi)^m} \int_{-\pi}^{\pi} \cdots \int_{-\pi}^{\pi} \left( \frac{\partial \langle H \rangle}{\partial \theta_j} \right)^2 d\theta_1 \cdots d\theta_m, j = 1, \dots, m. \end{aligned}$$

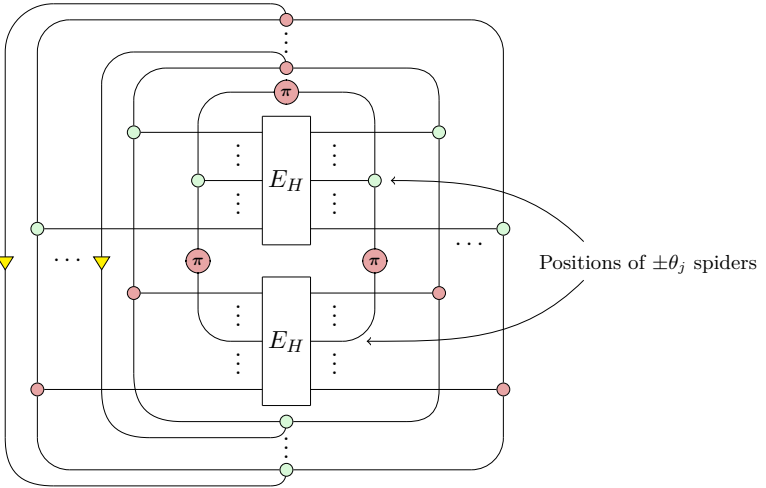
**Lemma 30.** Given  $\langle H \rangle$  in the form of (2), we have

$$\frac{1}{2\pi} \int_{-\pi}^{\pi} \left( \frac{\partial \langle H \rangle}{\partial \theta_j} \right)^2 d\theta_j =$$


where the cycle connects the legs of  $E_H$  that correspond to the positions of the  $\pm\theta_j$  spiders in (2).

**Remark 31.** The corresponding result given in [46] on page 12 is different from ours as shown in Lemma 30.

**Theorem 32.** Given  $\langle H \rangle$  in the form of (2), we have

$$\text{Var} \left( \frac{\partial \langle H \rangle}{\partial \theta_j} \right) =$$


*Proof.* We start from the diagram as shown in Lemma 30, then drag out variables iteratively according to Theorem 23, and the result follows.  $\square$

**Remark 33.** The variance computed in [46] is based on a sum over  $3^{m-1}$  terms ( $m$  is the number of parameters in the considered circuit), so when  $m$  is large it becomes infeasible to analyse the variance purely within ZX. Thus they have to resort to tensor networks which goes beyond the ZX method. In contrast, we avoid this exponential explosion by integrating without sums using algebraic ZX-calculus.

**Proposition 34.** Using the same  $\langle H \rangle$  as Example 28, we obtain the upper bound

$$\text{Var} \left( \frac{\partial \langle H \rangle}{\partial \theta_j} \right) = \frac{1}{(2\pi)^n} \int_{-\pi}^{\pi} \cdots \int_{-\pi}^{\pi} \left( \frac{\partial \langle H \rangle}{\partial \theta_j} \right)^2 d\theta_1 \cdots d\theta_n \leq \frac{1}{2^{n-2}}$$

for all  $j \in \{1, \dots, n\}$ . Thus, the ansatz from Example 27 suffers from barren plateaus.

*Proof.* By Theorem 32, we have

$$\text{Var} \left( \frac{\partial \langle H \rangle}{\partial \theta_j} \right) = \frac{1}{4^{n+1}} \pi \cdot \text{Diagram} \cdot \pi$$

The cycles in this diagram simplify as follows (see Lemmas 50 and 51):

Thus, we have

$$\text{Var} \left( \frac{\partial \langle H \rangle}{\partial \theta_j} \right) = \frac{1}{2^{n+2}} \pi \cdot \text{Diagram} \cdot \pi = \sum_{\vec{x} \in \{0,1\}^n} \frac{1}{2^{2n+2}} \pi \cdot \text{Diagram} \cdot \pi$$

Furthermore, we have  $\frac{x_1 \pi \cdots x_n \pi}{x_1 \pi \cdots x_n \pi} \leq 4$  for all  $\vec{x} \in \{0, 1\}^n$  (see Lemma 52), such that

$$\text{Var} \left( \frac{\partial \langle H \rangle}{\partial \theta_j} \right) \leq \sum_{\vec{x} \in \{0,1\}^n} 16 \frac{1}{2^{2n+2}} \pi = \frac{1}{2^{n-2}}. \quad \square$$

For further examples of barren plateau detection using Theorem 32 we refer to [28] where more ansätze from [37] as well as IQP ansätze [36] are analysed.

## 6 Conclusion and further work

We have elevated ZX-calculus from a graphical language for algebraic calculations to a new graphical tool for analytical reasoning. For example, it can now be used for tackling quantum optimisation problems and reasoning about quantum mechanics. We believe these techniques will extend the applicability of ZX-calculus to more problems related to quantum computing. With more work, ZX-calculus can become a general tool for graphical differential calculus.

There are many directions for future work:

1. **Generalisation of the results to qudit and qfinite cases [44]:** The ideas in this paper can be extended beyond qubits, giving us more diagrammatic analytical tools.
2. **Integrating arbitrary ZX diagrams:** This paper only gives the definite integral for circuit-like ZX diagrams. Indefinite integration of arbitrary ZX diagrams would in a sense complete the analytical ZX-calculus.
3. **Tool for automatic detection of barren plateaus in ansätze:** Interestingly, the variance diagram in Theorem 32 is mostly Clifford. This is exploited in [28] by contracting the diagram using ZX-based Clifford+T simulation algorithms [26, 27] to numerically detect barren plateaus. Further work on the contraction of such “Clifford+Triangle” diagrams could result in a tool that automatically detects barren plateaus in an ansatz without using a quantum computer.

## References

- [1] Gian-Luca R Anselmetti, David Wierichs, Christian Gogolin & Robert M Parrish (2021): *Local, expressive, quantum-number-preserving VQE ansätze for fermionic systems*. *New Journal of Physics* 23(11), p. 113010.
- [2] Miriam Backens & Ali Nabi Duman (2015): *A Complete Graphical Calculus for Spekkens’ Toy Bit Theory*. *Foundations of Physics* 46(1), p. 70–103, doi:10.1007/s10701-015-9957-7. Available at <http://dx.doi.org/10.1007/s10701-015-9957-7>.
- [3] Miriam Backens & Aleks Kissinger (2018): *ZH: A Complete Graphical Calculus for Quantum Computations Involving Classical Non-linearity*. In: *Proceedings of the 15th International Workshop on Quantum Physics and Logic, QPL 2018, Halifax, Canada, 3-7th June 2018.*, pp. 23–42. doi:10.4204/EPTCS.287.2.
- [4] Niel de Beaudrap, Xiaoning Bian & Quanlong Wang (2020): *Fast and Effective Techniques for T-Count Reduction via Spider Nest Identities*. In Steven T. Flammia, editor: *15th Conference on the Theory of Quantum Computation, Communication and Cryptography (TQC 2020), Leibniz International Proceedings in Informatics (LIPIcs)* 158, Schloss Dagstuhl–Leibniz-Zentrum für Informatik, Dagstuhl, Germany, pp. 11:1–11:23, doi:10.4230/LIPIcs.TQC.2020.11.
- [5] Niel de Beaudrap, Xiaoning Bian & Quanlong Wang (2020): *Techniques to reduce  $\pi/4$ -parity-phase circuits, motivated by the ZX calculus*. *Proceedings of the 16th International Conference on Quantum Physics and Logic 2019, EPTCS* 318, pp. 131–149. ArXiv:1911.09039.
- [6] Niel de Beaudrap & Dominic Horsman (2020): *The ZX calculus is a language for surface code lattice surgery*. *Quantum* 4, doi:10.22331/q-2020-01-09-218.

- [7] Hector Bombin, Chris Dawson, Ryan V Mishmash, Naomi Nickerson, Fernando Pastawski & Sam Roberts (2021): *Logical blocks for fault-tolerant topological quantum computation*. arXiv preprint arXiv:2112.12160.
- [8] Anna Choromanska, Mikael Henaff, Michael Mathieu, Gérard Ben Arous & Yann LeCun (2015): *The loss surfaces of multilayer networks*. In: *Artificial intelligence and statistics*, PMLR, pp. 192–204.
- [9] Bob Coecke & Ross Duncan (2008): *Interacting Quantum Observables*. In: *Automata, Languages and Programming*, 5126, Springer Berlin Heidelberg, pp. 298–310. [https://doi.org/10.1007/978-3-540-70583-3\\_25](https://doi.org/10.1007/978-3-540-70583-3_25).
- [10] Bob Coecke & Ross Duncan (2011): *Interacting quantum observables: categorical algebra and diagrammatics*. *New Journal of Physics* 13(4), p. 043016. Available at <http://stacks.iop.org/1367-2630/13/i=4/a=043016>. doi:10.1088/1367-2630/13/4/043016.
- [11] Bob Coecke, Ross Duncan, Aleks Kissinger & Quanlong Wang (2012): *Strong Complementarity and Non-locality in Categorical Quantum Mechanics*. In: *Proceedings of the 2012 27th Annual IEEE/ACM Symposium on Logic in Computer Science, LICS '12*, IEEE Computer Society, pp. 245–254. doi:10.1109/LICS.2012.35.
- [12] Bob Coecke & Bill Edwards (2012): *Spekkens's toy theory as a category of processes*. *Proceedings of Symposia in Applied Mathematics* 71, pp. 61–88.
- [13] Bob Coecke, Giovanni de Felice, Konstantinos Meichanetzidis & Alexis Toumi (2020): *Foundations for Near-Term Quantum Natural Language Processing*. Available at <https://arxiv.org/abs/2012.03755>.
- [14] Bob Coecke, Dominic Horsman, Aleks Kissinger & Quanlong Wang (2022): *Kindergarden quantum mechanics graduates ...or how I learned to stop gluing LEGO together and love the ZX-calculus*. *Theoretical Computer Science* 897, pp. 1–22, doi:<https://doi.org/10.1016/j.tcs.2021.07.024>. Available at <https://www.sciencedirect.com/science/article/pii/S0304397521004308>.
- [15] Bob Coecke & Aleks Kissinger (2010): *The Compositional Structure of Multipartite Quantum Entanglement*. In Samson Abramsky, Cyril Gavoille, Claude Kirchner, Friedhelm Meyer auf der Heide & Paul G. Spirakis, editors: *Automata, Languages and Programming*, Springer Berlin Heidelberg, Berlin, Heidelberg, pp. 297–308. doi:10.1007/978-3-642-14162-1\_25.
- [16] Bob Coecke, Aleks Kissinger, Alex Merry & Shibdas Roy (2011): *The GHZ/W-calculus contains rational arithmetic*. *Electronic Proceedings in Theoretical Computer Science* 52, p. 34–48, doi:10.4204/eptcs.52.4. Available at <http://dx.doi.org/10.4204/EPTCS.52.4>.
- [17] Ross Duncan, Aleks Kissinger, Simon Perdrix & John Van De Wetering (2020): *Graph-theoretic Simplification of Quantum Circuits with the ZX-calculus*. *Quantum* 4, p. 279.
- [18] Ross Duncan & Simon Perdrix (2010): *Rewriting measurement-based quantum computations with generalised flow*. In: *International Colloquium on Automata, Languages, and Programming*, Springer, pp. 285–296, doi:10.1007/978-3-642-14162-1\_24.
- [19] Stefano Gogioso & William Zeng (2019): *Generalised Mermin-type non-locality arguments*. *Logical Methods in Computer Science* Volume 15, Issue 2, doi:10.23638/LMCS-15(2:3)2019. Available at <https://lmcs.episciences.org/5402>.

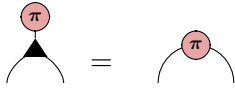
- [20] Amar Hadzihasanovic (2015): *A Diagrammatic Axiomatisation for Qubit Entanglement*. In: *2015 30th Annual ACM/IEEE Symposium on Logic in Computer Science*, pp. 573–584. doi:[10.1109/LICS.2015.59](https://doi.org/10.1109/LICS.2015.59).
- [21] Amar Hadzihasanovic, Kang Feng Ng & Quanlong Wang (2018): *Two Complete Axiomatisations of Pure-state Qubit Quantum Computing*. In: *Proceedings of the 33rd Annual ACM/IEEE Symposium on Logic in Computer Science*, LICS '18, ACM, pp. 502–511. doi:[10.1145/3209108.3209128](https://doi.org/10.1145/3209108.3209128).
- [22] Emmanuel Jeandel, Simon Perdrix & Margarita Veshchezerova (2022): *Addition and Differentiation of ZX-Diagrams*. In Amy P. Felty, editor: *7th International Conference on Formal Structures for Computation and Deduction, FSCD 2022, August 2-5, 2022, Haifa, Israel, LIPIcs 228*, Schloss Dagstuhl - Leibniz-Zentrum für Informatik, pp. 13:1–13:19, doi:[10.4230/LIPIcs.FSCD.2022.13](https://doi.org/10.4230/LIPIcs.FSCD.2022.13). Available at <https://doi.org/10.4230/LIPIcs.FSCD.2022.13>.
- [23] Dimitri Kartsaklis, Ian Fan, Richie Yeung, Anna Pearson, Robin Lorenz, Alexis Toumi, Giovanni de Felice, Konstantinos Meichanetzidis, Stephen Clark & Bob Coecke (2021): *lambeq: An Efficient High-Level Python Library for Quantum NLP*. arXiv preprint arXiv:2110.04236.
- [24] Aleks Kissinger (2022): *Phase-free ZX diagrams are CSS codes (... or how to graphically grok the surface code)*. arXiv preprint arXiv:2204.14038.
- [25] Aleks Kissinger & John van de Wetering (2019): *Universal MBQC with generalised parity-phase interactions and Pauli measurements*. *Quantum* 3, doi:[10.22331/q-2019-04-26-134](https://doi.org/10.22331/q-2019-04-26-134).
- [26] Aleks Kissinger & John van de Wetering (2022): *Simulating quantum circuits with ZX-calculus reduced stabiliser decompositions*. *Quantum Science and Technology*.
- [27] Aleks Kissinger, John van de Wetering & Renaud Vilmart (2022): *Classical simulation of quantum circuits with partial and graphical stabiliser decompositions*. arXiv preprint arXiv:2202.09202.
- [28] Mark Koch (2022): *Quantum Machine Learning using the ZXW-Calculus*. arXiv preprint arXiv:2210.11523.
- [29] Maciej Lewenstein (1994): *Quantum perceptrons*. *Journal of Modern Optics* 41(12), pp. 2491–2501.
- [30] Jin-Guo Liu, Yi-Hong Zhang, Yuan Wan & Lei Wang (2019): *Variational quantum eigensolver with fewer qubits*. *Phys. Rev. Research* 1, p. 023025, doi:[10.1103/PhysRevResearch.1.023025](https://doi.org/10.1103/PhysRevResearch.1.023025). Available at <https://link.aps.org/doi/10.1103/PhysRevResearch.1.023025>.
- [31] Robin Lorenz, Anna Pearson, Konstantinos Meichanetzidis, Dimitri Kartsaklis & Bob Coecke (2021): *Qnlp in practice: Running compositional models of meaning on a quantum computer*. arXiv preprint arXiv:2102.12846.
- [32] Jarrod R McClean, Sergio Boixo, Vadim N Smelyanskiy, Ryan Babbush & Hartmut Neven (2018): *Barren plateaus in quantum neural network training landscapes*. *Nature communications* 9(1), pp. 1–6.
- [33] Anthony Munson, Bob Coecke & Quanlong Wang (2020): *AND-gates in ZX-calculus: spider nest identities and QBC-completeness*. *Proceedings of the 17th International Conference on Quantum Physics and Logic (QPL) 2020*. arXiv:1910.06818.

- [34] John Preskill (2018): *Quantum Computing in the NISQ era and beyond*. *Quantum* 2, p. 79, doi:10.22331/q-2018-08-06-79. Available at <https://doi.org/10.22331/q-2018-08-06-79>.
- [35] Maria Schuld, Ville Bergholm, Christian Gogolin, Josh Izaac & Nathan Killoran (2019): *Evaluating analytic gradients on quantum hardware*. *Physical Review A* 99(3), p. 032331.
- [36] Dan Shepherd & Michael J Bremner (2009): *Temporally unstructured quantum computation*. *Proceedings of the Royal Society A: Mathematical, Physical and Engineering Sciences* 465(2105), pp. 1413–1439.
- [37] Sukin Sim, Peter D Johnson & Alán Aspuru-Guzik (2019): *Expressibility and entangling capability of parameterized quantum circuits for hybrid quantum-classical algorithms*. *Advanced Quantum Technologies* 2(12), p. 1900070.
- [38] Seyon Sivarajah, Silas Dilkes, Alexander Cowtan, Will Simmons, Alec Edgington & Ross Duncan (2020): *t|ket>: a retargetable compiler for NISQ devices*. *Quantum Science and Technology* 6(1), p. 014003.
- [39] Alexis Toumi, Richie Yeung & Giovanni de Felice (2021): *Diagrammatic Differentiation for Quantum Machine Learning*. In Chris Heunen & Miriam Backens, editors: *Proceedings 18th International Conference on Quantum Physics and Logic, QPL 2021, Gdansk, Poland, and online, 7-11 June 2021, EPTCS 343*, pp. 132–144, doi:10.4204/EPTCS.343.7. Available at <https://doi.org/10.4204/EPTCS.343.7>.
- [40] Quanlong Wang (2020): *An algebraic axiomatisation of ZX-calculus*. *Proceedings of the 17th International Conference on Quantum Physics and Logic (QPL) 2020*. arXiv:1911.06752.
- [41] Quanlong Wang (2020): *Algebraic complete axiomatisation of ZX-calculus with a normal form via elementary matrix operations*. arXiv:2007.13739v3.
- [42] Quanlong Wang (2020): *Completeness of algebraic ZX-calculus over arbitrary commutative rings and semirings*. arXiv:1912.01003v3.
- [43] Quanlong Wang (2021): *A non-anyonic qudit ZW-calculus*. arXiv:2109.11285.
- [44] Quanlong Wang (2021): *Qufinite ZX-calculus: a unified framework of qudit ZX-calculi*. arXiv:2104.06429.
- [45] Richie Yeung (2020): *Diagrammatic Design and Study of Ansatzes for Quantum Machine Learning*. arXiv preprint arXiv:2011.11073.
- [46] Chen Zhao & Xiao-Shan Gao (2021): *Analyzing the barren plateau phenomenon in training quantum neural networks with the ZX-calculus*. *Quantum* 5, p. 466, doi:10.22331/q-2021-06-04-466. Available at <https://doi.org/10.22331/q-2021-06-04-466>.

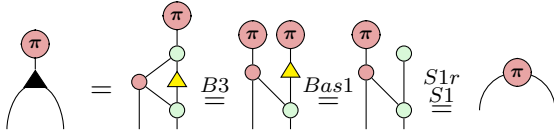
## A Proofs and Lemmas

In this appendix, we include all the lemmas with their proofs which have been essentially existed (up to scalars) in previous papers. The lemmas are given in the order which they appear in this paper.

**Lemma 10.**

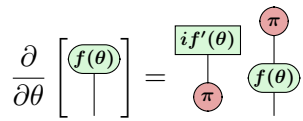


*Proof.*

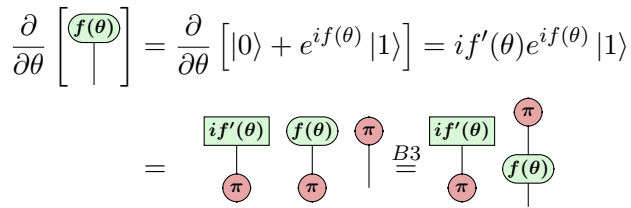


□

**Lemma 11.** Suppose  $f(\theta)$  is a differentiable real function of  $\theta$ . Then



*Proof.*

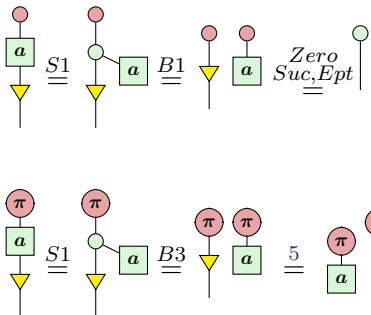


□

**Lemma 12.** For any complex number  $a$ , we have



*Proof.*



□

**Lemma 13.** Suppose  $f : \mathbb{R} \rightarrow \mathbb{C}$  is a differentiable function. If  $f(\theta) \neq 0$  for all  $\theta \in \mathbb{R}$ , then

$$\frac{\partial}{\partial \theta} \left[ \begin{array}{c} \boxed{f(\theta)} \\ | \\ \pi \end{array} \right] = \begin{array}{c} \boxed{\frac{f'(\theta)}{f(\theta)}} \\ | \\ \pi \end{array} \begin{array}{c} \pi \\ | \\ \boxed{f(\theta)} \end{array}$$

If  $f(\theta_0) = 0$  for some  $\theta_0 \in \mathbb{R}$ , then

$$\frac{\partial}{\partial \theta} \left[ \begin{array}{c} \boxed{f(\theta)} \\ | \\ \pi \end{array} \right]_{\theta_0} = \begin{array}{c} \pi \\ | \\ \boxed{f'(\theta_0)} \end{array}$$

*Proof.*

$$\begin{aligned} \frac{\partial}{\partial \theta} \left[ \begin{array}{c} \boxed{f(\theta)} \\ | \\ \pi \end{array} \right] &= \frac{\partial}{\partial \theta} [|0\rangle + f(\theta) |1\rangle] = f'(\theta) |1\rangle \\ &= \begin{array}{c} \boxed{f'(\theta)} \\ | \\ \pi \end{array} \begin{array}{c} \pi \\ | \\ \pi \end{array} \end{aligned}$$

If  $f(\theta) \neq 0$  for all  $\theta \in \mathbb{R}$ , then

$$\begin{array}{c} \boxed{f'(\theta)} \\ | \\ \pi \end{array} \begin{array}{c} \pi \\ | \\ \pi \end{array} = \begin{array}{c} \boxed{\frac{f'(\theta)}{f(\theta)}} \\ | \\ \pi \end{array} \begin{array}{c} \boxed{f(\theta)} \\ | \\ \pi \end{array} \begin{array}{c} \pi \\ | \\ \pi \end{array} = \begin{array}{c} \boxed{\frac{f'(\theta)}{f(\theta)}} \\ | \\ \pi \end{array} \begin{array}{c} \pi \\ | \\ \boxed{f(\theta)} \end{array}$$

If  $f(\theta_0) = 0$  for some  $\theta_0 \in \mathbb{R}$ , then

$$\begin{array}{c} \boxed{f'(\theta_0)} \\ | \\ \pi \end{array} \begin{array}{c} \pi \\ | \\ \pi \end{array} = \begin{array}{c} \pi \\ | \\ \boxed{f'(\theta_0)} \end{array}$$

□

**Lemma 35.**

$$\boxed{0} = \begin{array}{c} \pi \\ | \\ \pi \end{array}$$

*Proof.*

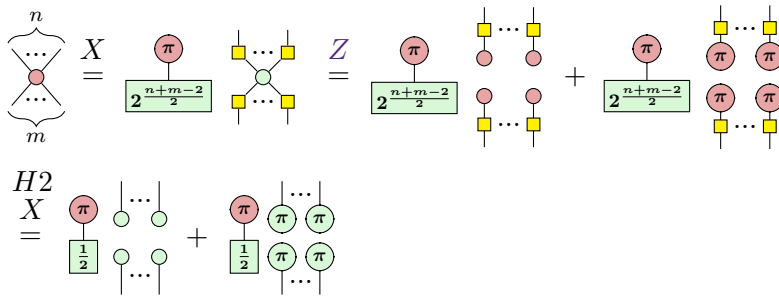
$$\boxed{0} \stackrel{S1}{=} \boxed{0} \begin{array}{c} \pi \\ | \\ \pi \end{array} \stackrel{Zero}{=} \begin{array}{c} \pi \\ | \\ \pi \end{array} \begin{array}{c} \pi \\ | \\ \pi \end{array} \stackrel{B1}{=} \begin{array}{c} \pi \\ | \\ \pi \end{array}$$

□

**Lemma 36.**

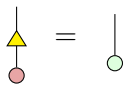
$$\begin{array}{c} \dots \\ \diagdown \quad \diagup \\ \pi \\ \diagup \quad \diagdown \\ \dots \end{array} = \begin{array}{c} \pi \\ | \\ \frac{1}{2} \end{array} \begin{array}{c} \dots \\ | \\ \pi \end{array} \begin{array}{c} \dots \\ | \\ \pi \end{array} + \begin{array}{c} \pi \\ | \\ \frac{1}{2} \end{array} \begin{array}{c} \pi \\ | \\ \pi \end{array} \begin{array}{c} \dots \\ | \\ \pi \end{array}$$

*Proof.*

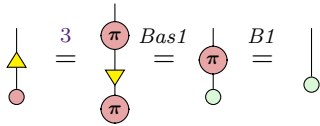


□

**Lemma 37.**

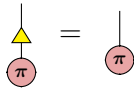


*Proof.*

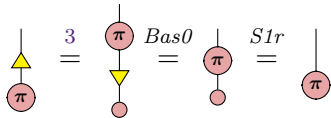


□

**Lemma 38.**

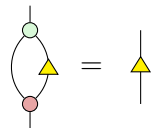


*Proof.*

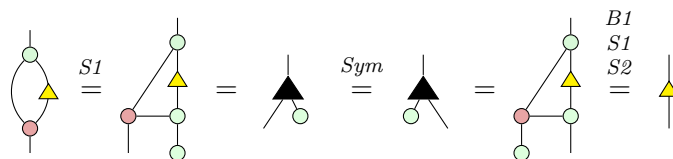


□

**Lemma 39.**

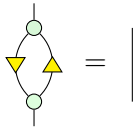


*Proof.*

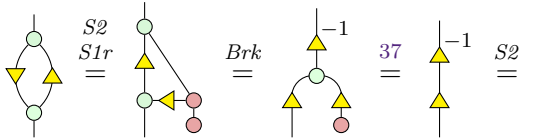


□

**Lemma 40.**

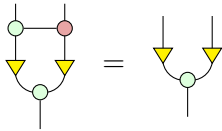


*Proof.*

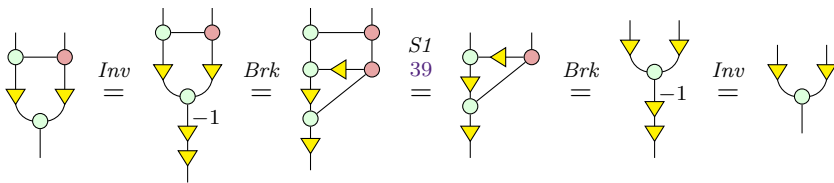


□

**Lemma 41.**

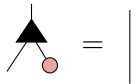


*Proof.*

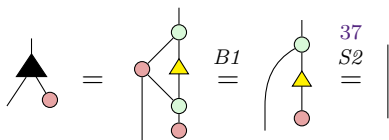


□

**Lemma 42.**

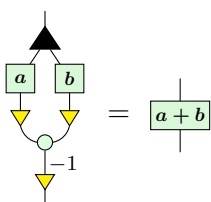


*Proof.*

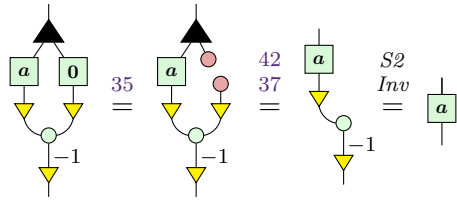


□

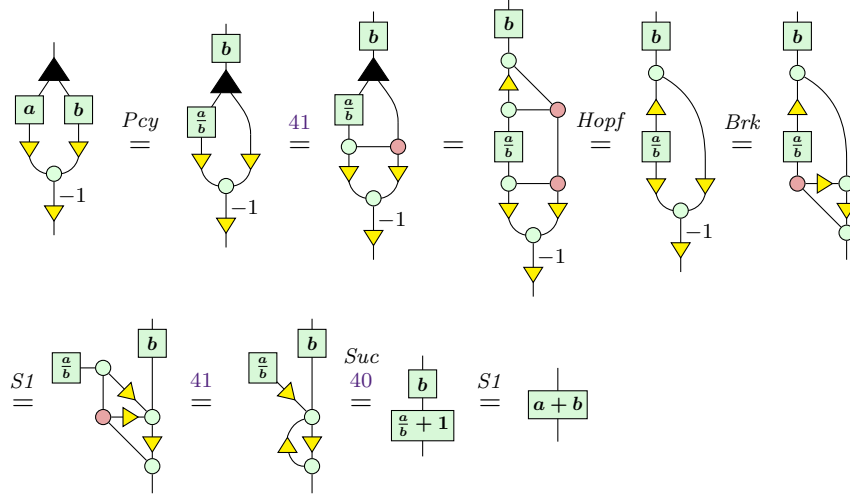
**Lemma 43.** *Let  $a, b \in \mathbb{C}$ . Then*



*Proof.* If  $b = 0$ , then

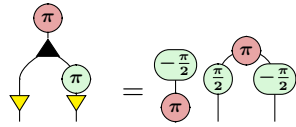


If  $b \neq 0$ , then

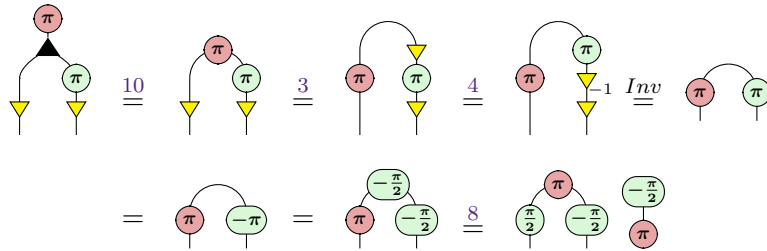


□

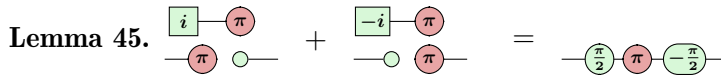
**Lemma 44.**



*Proof.*



□



*Proof.* We use the triangle to do the change of basis from  $|+\rangle$  and  $|1\rangle$  to  $|0\rangle$  and  $|1\rangle$ .

$$\begin{array}{c}
 \begin{array}{c} \boxed{i} \quad \pi \\ \hline \pi \quad \circ \end{array} + \begin{array}{c} \boxed{-i} \quad \pi \\ \hline \circ \quad \pi \end{array} \\
 \\
 \stackrel{5, Suc}{\underline{Zero}} \begin{array}{c} \boxed{i} \quad \pi \\ \hline \pi \quad \circ \end{array} \leftarrow \begin{array}{c} \boxed{-i} \quad \pi \\ \hline \circ \quad \pi \end{array} \rightarrow = \begin{array}{c} \boxed{i} \quad \pi \\ \hline \pi \quad \circ \quad \pi \end{array} \leftarrow \begin{array}{c} \boxed{i} \quad \pi \\ \hline \circ \quad \pi \end{array} \rightarrow \\
 \\
 \stackrel{B1}{\underline{B3}} \begin{array}{c} \boxed{i} \\ \hline \pi \end{array} \leftarrow \begin{array}{c} \circ \\ \hline \pi \end{array} \rightarrow + \begin{array}{c} \boxed{i} \\ \hline \pi \end{array} \leftarrow \begin{array}{c} \circ \\ \hline \pi \end{array} \rightarrow = \begin{array}{c} \boxed{i} \\ \hline \pi \end{array} \leftarrow \begin{array}{c} \circ \\ \hline \pi \end{array} \rightarrow
 \end{array}$$

The rest of the proof is identical to the proof of Lemma 44. □

**Lemma 46.**

$$\begin{array}{c} \circ \quad \circ \\ \hline \pi \end{array} = \begin{array}{c} \pi \\ \hline \circ \end{array}$$

*Proof.*

$$\begin{array}{c} \circ \quad \circ \\ \hline \pi \end{array} \stackrel{S1}{=} \begin{array}{c} \circ \quad \circ \\ \hline \pi \end{array} \xrightarrow{Hopf} \begin{array}{c} \circ \quad \circ \\ \hline \pi \end{array} \stackrel{S1r}{\underline{S2}} = \begin{array}{c} \pi \\ \hline \circ \end{array}$$

□

**Lemma 47.**

$$\begin{array}{c} \circ \\ \hline \pi \\ \hline \circ \quad \circ \end{array} = \begin{array}{c} \pi \\ \hline \pi \\ \hline \circ \quad \circ \end{array}$$

*Proof.*

$$\begin{array}{c} \circ \\ \hline \pi \\ \hline \circ \quad \circ \end{array} \stackrel{S1}{=} \begin{array}{c} \circ \\ \hline \pi \\ \hline \circ \quad \circ \end{array} \xrightarrow{Pic} \begin{array}{c} \pi \\ \hline \pi \\ \hline \circ \quad \circ \end{array} \stackrel{S1}{=} \begin{array}{c} \pi \\ \hline \pi \\ \hline \circ \quad \circ \end{array} \xrightarrow{Hopf} \begin{array}{c} \pi \\ \hline \pi \\ \hline \circ \quad \circ \end{array}$$

□

**Lemma 48.**

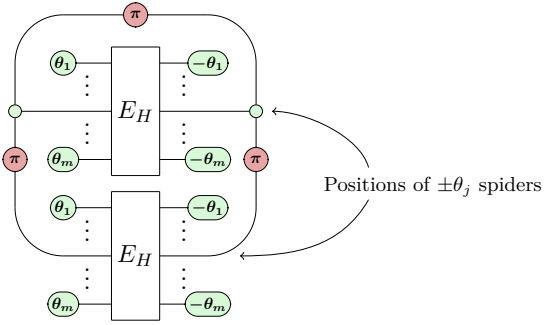
$$\begin{array}{c} \pi \\ \hline \pi \\ \hline \circ \quad \circ \end{array} = \begin{array}{c} \pi \\ \hline \pi \\ \hline \circ \quad \circ \end{array}$$

*Proof.*

$$\begin{array}{c} \pi \\ \hline \pi \\ \hline \circ \quad \circ \end{array} \stackrel{S1}{=} \begin{array}{c} \pi \\ \hline \pi \\ \hline \circ \quad \circ \end{array} \xrightarrow{Pic} \begin{array}{c} \pi \\ \hline \pi \\ \hline \circ \quad \circ \end{array} \stackrel{S1}{=} \begin{array}{c} \pi \\ \hline \pi \\ \hline \circ \quad \circ \end{array}$$

□

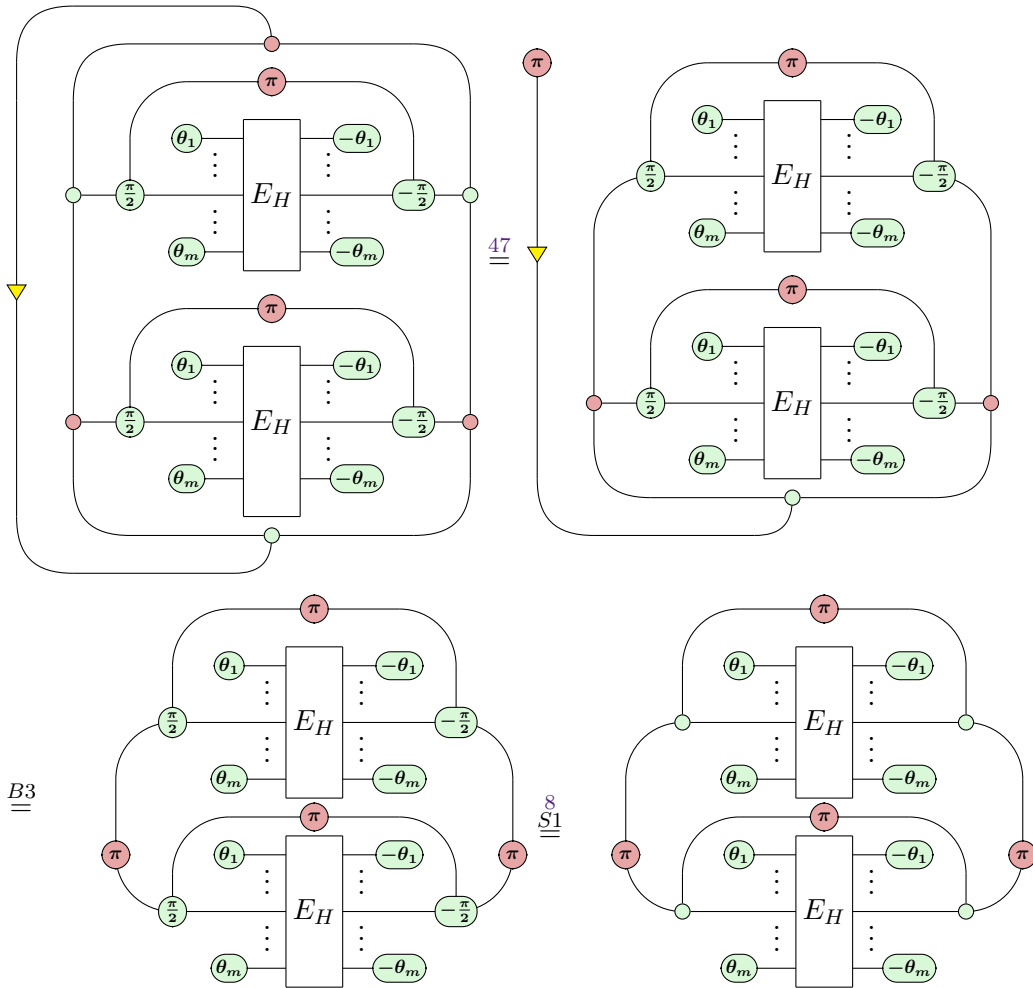
**Lemma 30.** Given  $\langle H \rangle$  in the form of (2), we have

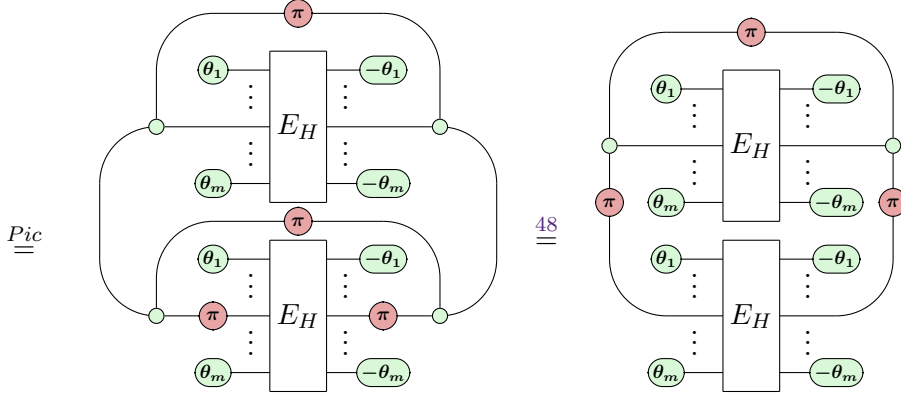
$$\frac{1}{2\pi} \int_{-\pi}^{\pi} \left( \frac{\partial \langle H \rangle}{\partial \theta_j} \right)^2 d\theta_j =$$


where the cycle connects the legs of  $E_H$  that correspond to the positions of the  $\pm\theta_j$  spiders in (2).

*Proof.* By Theorem 23,

$$\frac{1}{2\pi} \int_{-\pi}^{\pi} \left( \frac{\partial \langle H \rangle}{\partial \theta_j} \right)^2 d\theta_j =$$





□

## B Integration proofs

**Proposition 20.** Let  $k$  be an arbitrary non-zero integer,  ${}^{m+1} \left\{ \begin{array}{c} \vdots \\ K \\ \vdots \end{array} \right\}^{n+1}$  be any ZX diagram with  $m, n \geq 0$  which has no occurrence of  $\alpha$ . Then

$$\frac{1}{2\pi} \int_{-\pi}^{\pi} {}^m \left\{ \begin{array}{c} \overset{k\alpha}{\vdots} \\ K \\ \underset{-k\alpha}{\vdots} \end{array} \right\}^n d\alpha = {}^m \left\{ \begin{array}{c} \vdots \\ K \\ \vdots \end{array} \right\}^n$$

*Proof.*

$$\begin{aligned} {}^m \left\{ \begin{array}{c} \overset{k\alpha}{\vdots} \\ K \\ \underset{-k\alpha}{\vdots} \end{array} \right\}^n &= \left( (\langle 0| + e^{-ik\alpha} \langle 1|) \otimes I^{\otimes n} \right) K \left( (|0\rangle + e^{ik\alpha} |1\rangle) \otimes I^{\otimes m} \right) \\ &= (\langle 0| \otimes I^{\otimes n}) K (|0\rangle \otimes I^{\otimes m}) + e^{ik\alpha} (\langle 0| \otimes I^{\otimes n}) K (|1\rangle \otimes I^{\otimes m}) \\ &\quad + e^{-ik\alpha} (\langle 1| \otimes I^{\otimes n}) K (|0\rangle \otimes I^{\otimes m}) + (\langle 1| \otimes I^{\otimes n}) K (|1\rangle \otimes I^{\otimes m}) \end{aligned}$$

We have  $\frac{1}{2\pi} \int_{-\pi}^{\pi} e^{ik\alpha} d\alpha = \frac{2 \sin(k\pi)}{k} = 0$  for all non-zero integers  $k$ . Therefore

$$\frac{1}{2\pi} \int_{-\pi}^{\pi} {}^m \left\{ \begin{array}{c} \overset{k\alpha}{\vdots} \\ K \\ \underset{-k\alpha}{\vdots} \end{array} \right\}^n d\alpha = (\langle 0| \otimes I^{\otimes n}) K (|0\rangle \otimes I^{\otimes m}) + (\langle 1| \otimes I^{\otimes n}) K (|1\rangle \otimes I^{\otimes m})$$

$$\begin{aligned}
&= m \left\{ \begin{array}{c} \vdots \\ K \\ \vdots \end{array} \right\}_n + m \left\{ \begin{array}{c} \vdots \\ K \\ \vdots \end{array} \right\}_n = m \left\{ \begin{array}{c} \vdots \\ K \\ \vdots \end{array} \right\}_n + m \left\{ \begin{array}{c} \vdots \\ K \\ \vdots \end{array} \right\}_n \\
&= \left( \text{diagram with red and green dots} \right) + \left( \text{diagram with red and green dots} \right) \\
&= \left( \text{diagram with red and green dots} \right) = \left( \text{diagram with red and green dots} \right)
\end{aligned}$$

□

**Lemma 49.**

$$\begin{array}{c} \bullet \\ \bullet \end{array} + \begin{array}{c} \pi \\ \bullet \end{array} = \text{diagram with red and green dots}$$

*Proof.*

$$\begin{array}{c} \bullet \\ \bullet \end{array} + \begin{array}{c} \pi \\ \bullet \end{array} \stackrel{\text{Bas0}}{\underset{\text{Bas1}}{=}} \begin{array}{c} \bullet \\ \bullet \end{array} + \begin{array}{c} \pi \\ \bullet \end{array} = \text{diagram with red and green dots} = \text{diagram with red and green dots} = \text{diagram with red and green dots}$$

□

**Theorem 23.** Let  $k$  be an arbitrary non-zero integer,  ${}_{m+2} \left\{ \begin{array}{c} \vdots \\ A \\ \vdots \end{array} \right\}_{n+2}$  be any ZX diagram with  $m, n \geq 0$  which has no occurrence of  $\alpha$ . Then

$$\frac{1}{2\pi} \int_{-\pi}^{\pi} \begin{array}{c} k\alpha \\ k\alpha \\ \vdots \\ A \\ \vdots \\ -k\alpha \\ -k\alpha \end{array} d\alpha = \text{diagram with red and green dots}$$

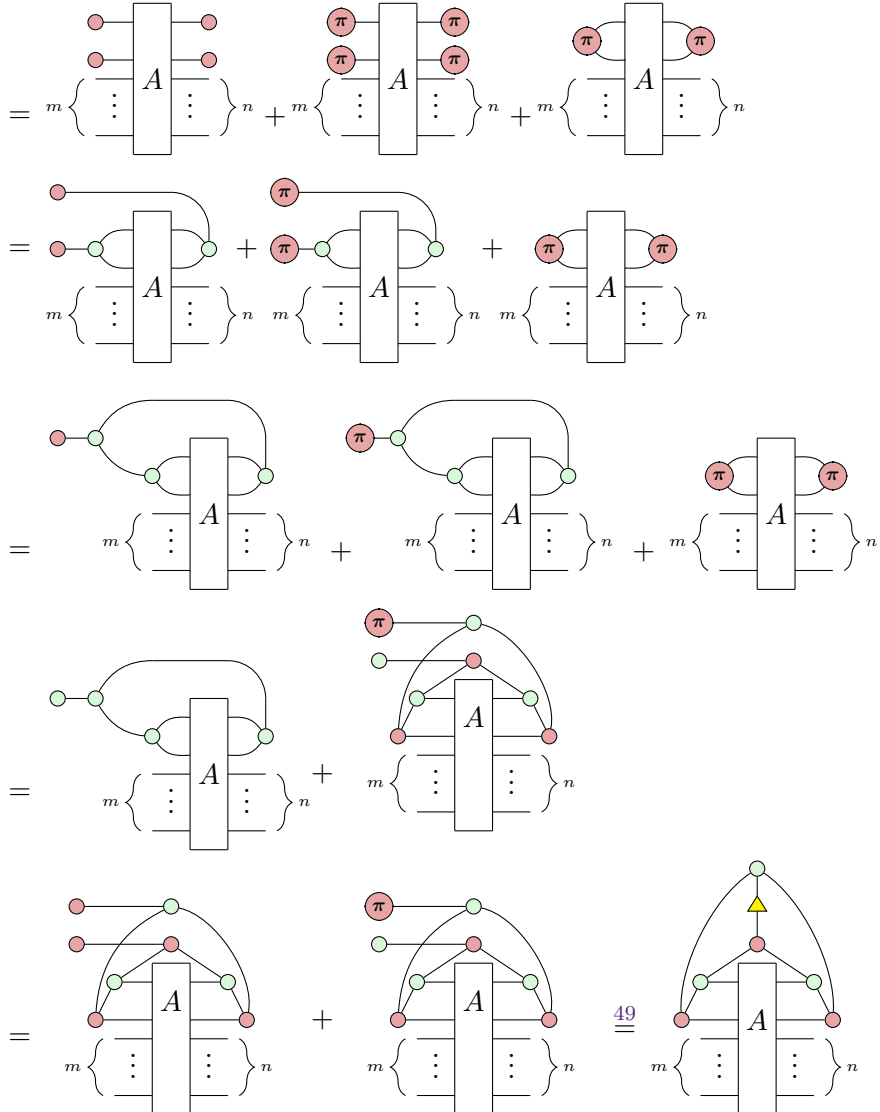
*Proof.*

$$\begin{aligned}
F &= \begin{array}{c} k\alpha \\ k\alpha \\ \vdots \\ A \\ \vdots \\ -k\alpha \\ -k\alpha \end{array} \\
&= \left[ \left( \langle 0| + e^{-ik\alpha} \langle 1| \right) \otimes \left( \langle 0| + e^{-ik\alpha} \langle 1| \right) \otimes I^{\otimes n} \right] A \left[ \left( |0\rangle + e^{ik\alpha} |1\rangle \right) \otimes \left( |0\rangle + e^{ik\alpha} |1\rangle \right) \otimes I^{\otimes m} \right]
\end{aligned}$$

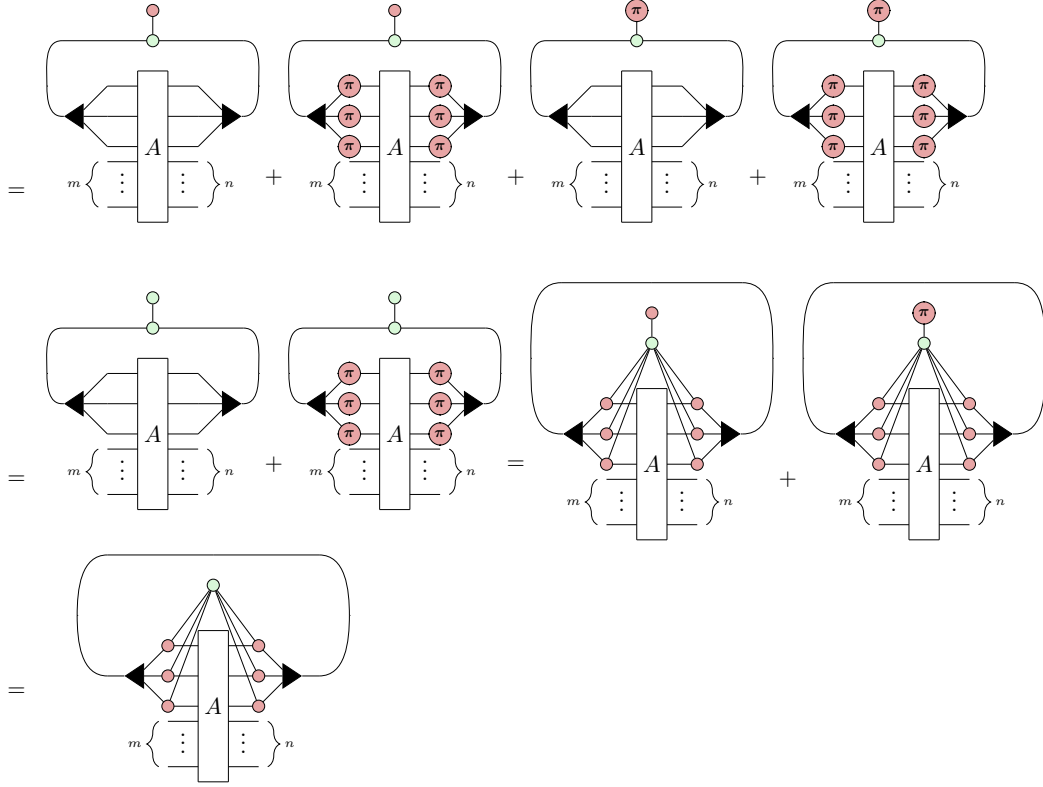
$$\begin{aligned}
&= \left[ \left( \langle 00| + e^{-ik\alpha} \langle 01| + \langle 10| + e^{-i2k\alpha} \langle 11| \right) \otimes I^{\otimes n} \right] A \left[ \left( |00\rangle + e^{ik\alpha} (|01\rangle + |10\rangle) \right. \right. \\
&\quad \left. \left. + e^{i2k\alpha} |11\rangle \right) \otimes I^{\otimes m} \right] \\
&= (\langle 00| \otimes I^{\otimes n}) A (|00\rangle \otimes I^{\otimes m}) + (\langle 11| \otimes I^{\otimes n}) A (|11\rangle \otimes I^{\otimes m}) \\
&\quad + ((\langle 01| + \langle 10|) \otimes I^{\otimes n}) A ((|01\rangle + |10\rangle) \otimes I^{\otimes m}) \\
&\quad + e^{ik\alpha} (\langle 00| \otimes I^{\otimes n}) A ((|01\rangle + |10\rangle) \otimes I^{\otimes m}) \\
&\quad + e^{i2k\alpha} (\langle 00| \otimes I^{\otimes n}) A (|11\rangle \otimes I^{\otimes m}) \\
&\quad + e^{-ik\alpha} ((\langle 01| + \langle 10|) \otimes I^{\otimes n}) A (|00\rangle \otimes I^{\otimes m}) \\
&\quad + e^{-ik\alpha} (\langle 11| \otimes I^{\otimes n}) A ((|01\rangle + |10\rangle) \otimes I^{\otimes m}) \\
&\quad + e^{-i2k\alpha} (\langle 11| \otimes I^{\otimes n}) A (|00\rangle \otimes I^{\otimes m}) \\
&\quad + e^{ik\alpha} ((\langle 01| + \langle 10|) \otimes I^{\otimes n}) A (|11\rangle \otimes I^{\otimes m})
\end{aligned}$$

We have  $\frac{1}{2\pi} \int_{-\pi}^{\pi} e^{ik\alpha} d\alpha = \frac{2\sin(k\pi)}{k} = 0$  for all non-zero integers  $k$ . Therefore

$$\begin{aligned}
\frac{1}{2\pi} \int_{-\pi}^{\pi} F d\alpha &= (\langle 00| \otimes I^{\otimes n}) A (|00\rangle \otimes I^{\otimes m}) + (\langle 11| \otimes I^{\otimes n}) A (|11\rangle \otimes I^{\otimes m}) \\
&\quad + ((\langle 01| + \langle 10|) \otimes I^{\otimes n}) A ((|01\rangle + |10\rangle) \otimes I^{\otimes m})
\end{aligned}$$







□

## C Barren Plateau Analysis

**Lemma 29.** Given  $\langle H \rangle$  in the form of (2), we have  $\mathbf{E} \left( \frac{\partial \langle H \rangle}{\partial \theta_j} \right) = 0$ , for  $j = 1, \dots, m$ .

*Proof.* By integrating over the uniform distribution, we have

$$\mathbf{E} \left( \frac{\partial \langle H \rangle}{\partial \theta_j} \right) = \frac{1}{(2\pi)^m} \int_{-\pi}^{\pi} \dots \int_{-\pi}^{\pi} \frac{\partial \langle H \rangle}{\partial \theta_j} d\theta_1 \dots d\theta_m.$$

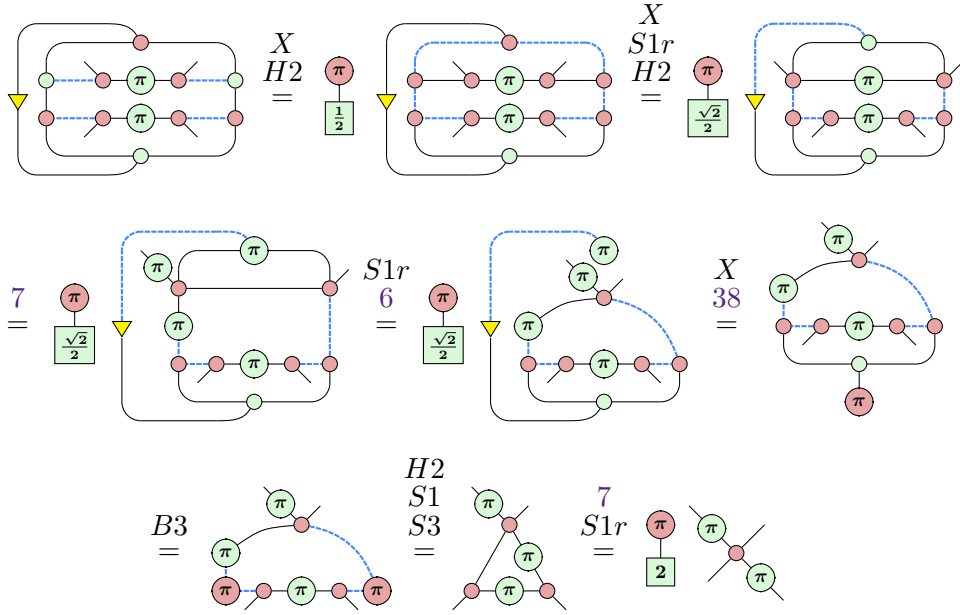
We prove the theorem by showing that  $\frac{1}{2\pi} \int_{-\pi}^{\pi} \frac{\partial \langle H \rangle}{\partial \theta_j} d\theta_j = 0$ .

$$\frac{\partial \langle H \rangle}{\partial \theta_j} \stackrel{18}{=} \begin{array}{c} \text{Diagram 1: A central vertical bar labeled } E_H \text{ with } m \text{ horizontal lines. The top line has a red circle labeled } \pi \text{ above it. The } j \text{-th line from the top has a green circle labeled } \theta_j \text{ on the left and } -\theta_j \text{ on the right. The } m \text{-th line from the top has a green circle labeled } \theta_m \text{ on the left and } -\theta_m \text{ on the right. The } j \text{-th line from the bottom has a green circle labeled } -\theta_j \text{ on the left and } \theta_j \text{ on the right. The } m \text{-th line from the bottom has a green circle labeled } -\theta_m \text{ on the left and } \theta_m \text{ on the right. The } j \text{-th and } m \text{-th lines are connected by arcs at the top and bottom.} \end{array}$$

$$\frac{1}{2\pi} \int_{-\pi}^{\pi} \frac{\partial \langle H \rangle}{\partial \theta_j} d\theta_j \stackrel{20}{=} \begin{array}{c} \text{Diagram 2: A central vertical bar labeled } E_H \text{ with } m \text{ horizontal lines. The top line has a red circle labeled } \pi \text{ above it. The } j \text{-th line from the top has a green circle labeled } \theta_j \text{ on the left and } -\theta_j \text{ on the right. The } m \text{-th line from the top has a green circle labeled } \theta_m \text{ on the left and } -\theta_m \text{ on the right. The } j \text{-th and } m \text{-th lines are connected by arcs at the top and bottom.} \end{array}$$



Proof.



□

**Lemma 52.** For all  $x \in \{0, 1\}^n$ , we have

$$\begin{array}{c} \textcircled{x_1 \pi} \cdots \textcircled{x_n \pi} \\ \textcircled{x_1 \pi} \cdots \textcircled{x_n \pi} \end{array} \leq 4$$

Proof. By induction on  $n$ . For  $n = 1$ , we have

$$\begin{array}{c} \textcircled{x_1 \pi} \\ \textcircled{x_1 \pi} \end{array} = \begin{cases} 4 & \text{if } x_1 = 0, \\ 0 & \text{if } x_1 = 1. \end{cases}$$

For  $n = 2$ , we have

$$\begin{array}{c} \textcircled{x_1 \pi} \cdots \textcircled{x_2 \pi} \\ \textcircled{x_1 \pi} \cdots \textcircled{x_2 \pi} \end{array} \stackrel{X}{=} \begin{array}{c} \textcircled{\pi} \\ \boxed{2} \end{array} \begin{array}{c} \textcircled{x_1 \pi} \textcircled{x_2 \pi} \\ \textcircled{x_1 \pi} \textcircled{x_2 \pi} \end{array} = 2.$$

In the inductive case  $n > 2$ , we have

$$\begin{array}{c} \textcircled{x_1 \pi} \cdots \textcircled{x_n \pi} \textcircled{x_{n+1} \pi} \textcircled{x_{n+2} \pi} \\ \textcircled{x_1 \pi} \cdots \textcircled{x_n \pi} \textcircled{x_{n+1} \pi} \textcircled{x_{n+2} \pi} \end{array} \stackrel{X}{=} \begin{array}{c} \textcircled{x_1 \pi} \cdots \textcircled{x_n \pi} \textcircled{x_{n+1} \pi} \textcircled{x_{n+2} \pi} \\ \textcircled{x_1 \pi} \cdots \textcircled{x_n \pi} \textcircled{x_{n+1} \pi} \textcircled{x_{n+2} \pi} \end{array}$$

$$\stackrel{B_1}{=} \stackrel{B_3}{=} \begin{array}{c} \textcircled{x_1 \pi} \cdots \textcircled{(x_n + x_{n+2}) \pi} \\ \textcircled{x_1 \pi} \cdots \textcircled{(x_n + x_{n+2}) \pi} \end{array} \stackrel{\text{IH}}{\leq} 4$$

where the inductive hypothesis is applied with  $\vec{x} = (x_1, \dots, x_{n-1}, x_n + x_{n+2})$ . □

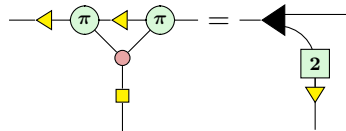
## D Comparison with Jeandel et al.

Jeandel, Perdrix, and Veshchezerova present an alternate method to represent derivatives with the ZX-calculus [22]. We want to show that the two papers arrive at similar results through very different techniques, and that some results in [22] can be more compactly represented by explicitly using

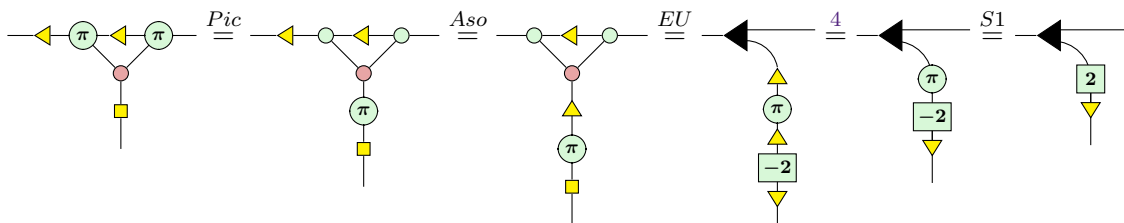
the W spider. The nodes used in [22] are similar to ours: the circle green nodes, the Hadamard node and the red nodes are exactly the same, but we additionally have pink nodes which are different to the red nodes up to a variational scalar, and have green box nodes which have the circle green nodes as special cases while can be turned into circle green nodes with the help of the yellow triangle node [21]. Also note that their black triangle corresponds to our yellow triangle and our black triangle corresponds to the W spider.

First, we show that the triangular-shaped diagram that features in their differentiation result can be represented compactly using the W spider:

**Lemma 53.**

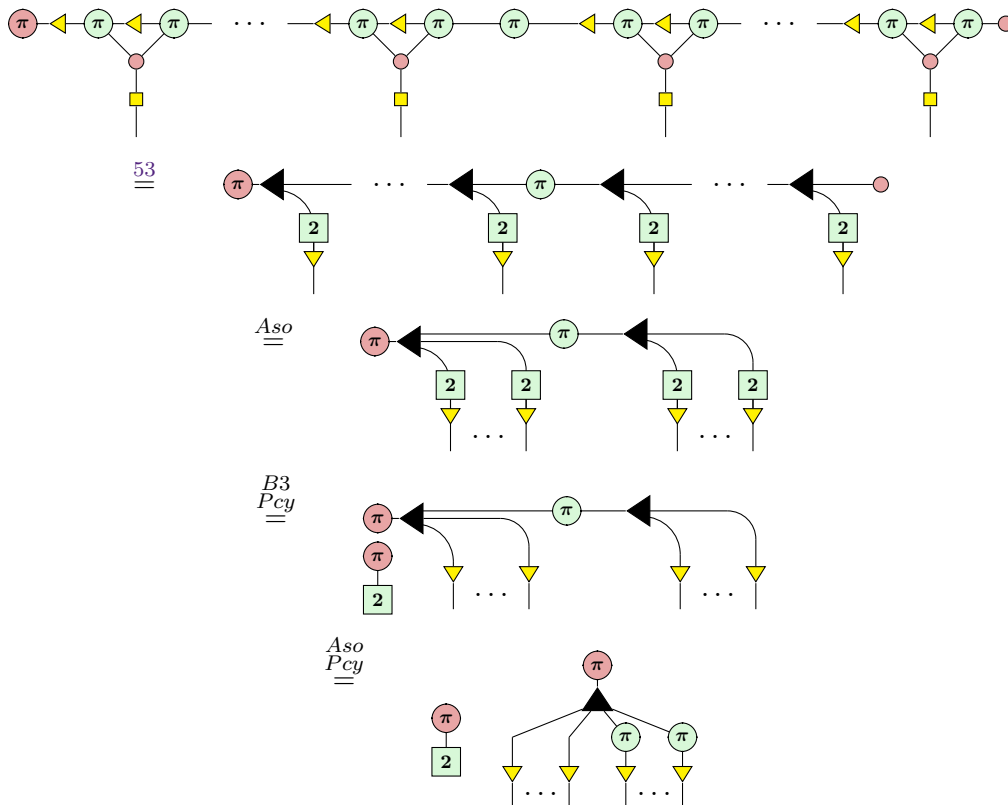


*Proof.*



□

**Remark 54.** The differentiation of “linear” ZX diagrams result obtained by [22] is equivalent to our lemma 17.

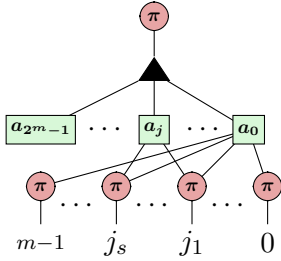


Although the end results are equivalent, we emphasise that their result is obtained through their theory of summing controlled diagrams, whilst our result is obtained through our arbitrary differentiation result.

**Remark 55.** The general differentiation result in [22] requires an inductive conversion to controlled diagrams, and is obtained through combining diagrammatic addition and the Leibniz product rule. Because of this, the resulting diagram will not resemble the original diagram.

In comparison, our Theorem 14 does not affect the topology of the original diagram and can be calculated almost instantly.

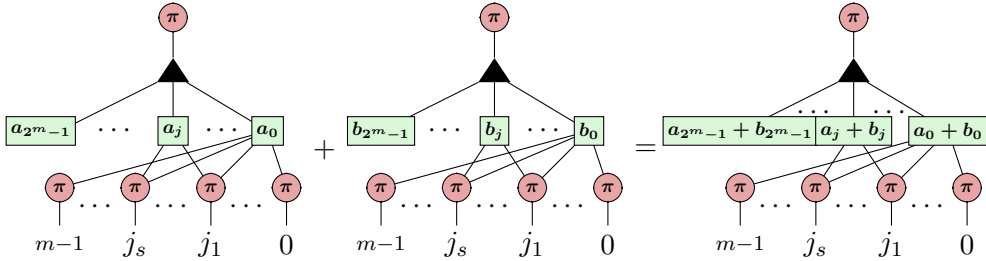
**Remark 56.** Both the general results on addition of diagrams and on differentiation of diagrams shown in [22] are based on induction on generators. If such induction methods are allowed, then there is an alternative way to generally add two ZX diagrams or differentiate a ZX diagram: first rewrite inductively the diagrams into the compressed normal form shown in [41] as follows



which corresponding to the vector

$$\begin{pmatrix} a_0 \\ a_1 \\ \vdots \\ a_{2^{m-2}} \\ a_{2^{m-1}} \end{pmatrix},$$

then the sum of two diagrams can be obtained by adding up the corresponding parameters in the two diagrams:



and the differentiation can be obtained element-wisely:

